

Review

Recent Progress and Challenges Regarding Magnetite-Based Nanoparticles for Targeted Drug Delivery

Joanna Kurczewska ^{1,*}  and Bernadeta Dobosz ² ¹ Faculty of Chemistry, Adam Mickiewicz University, Uniwersytetu Poznańskiego 8, 61-614 Poznań, Poland² Faculty of Physics, Adam Mickiewicz University, Uniwersytetu Poznańskiego 2, 61-614 Poznań, Poland; benia@amu.edu.pl

* Correspondence: asiaw@amu.edu.pl; Tel.: +48-61-829-1565

Abstract: Magnetite-based nanoparticles are of constant interest in the scientific community as potential systems for biomedical applications. Over the years, the ability to synthesize diverse systems based on iron (II, III) oxide nanoparticles has been mastered to maximize their potential effectiveness in the targeted delivery of active substances in cancer therapy. The present review explores recent literature findings that detail various magnetic nanosystems. These encompass straightforward designs featuring a polymer coating on the magnetic core and more intricate matrices for delivering chemotherapeutic drugs. This paper emphasizes novel synthetic approaches that impact the efficacy and progress of anticancer investigations, specifically targeting a particular cancer type. The research also delves into combinations with alternative treatment methods and diagnostic approaches. Additionally, it highlights a critical aspect—the interaction with cells—identifying it as the least developed aspect in current research on these systems.

Keywords: magnetite; targeted drug delivery; chemotherapy; multifunctional nanosystems



Citation: Kurczewska, J.; Dobosz, B. Recent Progress and Challenges Regarding Magnetite-Based Nanoparticles for Targeted Drug Delivery. *Appl. Sci.* **2024**, *14*, 1132. <https://doi.org/10.3390/app14031132>

Academic Editors: Francesca Brero and Manuel Mariani

Received: 18 December 2023

Revised: 25 January 2024

Accepted: 27 January 2024

Published: 29 January 2024



Copyright: © 2024 by the authors. Licensee MDPI, Basel, Switzerland. This article is an open access article distributed under the terms and conditions of the Creative Commons Attribution (CC BY) license (<https://creativecommons.org/licenses/by/4.0/>).

1. Introduction

Magnetic materials are a specific group characterized by unique properties that can be utilized in different technologies, including biomedical applications. An extensive group of research on magnetic materials concerns nanomaterials with external dimensions not exceeding 100 nm. Magnetic nanomaterials can be categorized into two general groups—metals and their compounds (alloys, oxides, ferrites) [1]. Particular attention is paid to systems based on magnetic iron oxide nanomaterials, dominated by systems based on iron (II, III) oxide (Fe₃O₄, magnetite).

Magnetite differs from other iron oxides as it contains divalent and trivalent iron. The mixture of Fe²⁺ and Fe³⁺ is present at the octahedral site and surrounded by six oxygen atoms, while only Fe³⁺ ions surrounded by four oxygen atoms occupy the tetrahedral site. Magnetite is ferromagnetic and demonstrates high electrical conductivity [2].

Over the years, many methods have been developed to obtain magnetite nanoparticles (Table 1) [3–7]. When designing a new material for a specific application, choosing a method that would guarantee obtaining magnetite nanoparticles of a specific shape, size, and crystallinity would be necessary. Unfortunately, each method has drawbacks and limitations, so choosing the most optimal one depends on the target expectations. Here, we briefly describe some of the most often applied methods. The most common and simple technique is coprecipitation, which requires two components—precursors in the form of iron salts (Fe²⁺/Fe³⁺) and a precipitation agent (NH₄OH, NaOH, or KOH) [8]. The shape and the size of NPs depend on the type of salts, temperature, pH, stirring speed, and ionic strength. Procedures for this method often include using an inert gas to prevent the transformation of magnetite into maghemite and additives (e.g., citric acid) to prevent agglomeration and the formation of larger particles. Depending on the protocol used, the

coprecipitation method allows for obtaining nanoparticles of uniform sizes, often below 10 nm, but many reports indicate a significant variation in sizes (10–40 nm). Another popular technique is hydrothermal synthesis, which uses high temperature (>200 °C) and high pressure (>6000 Pa) in a reactor to obtain uniform and homogeneous crystals. The modification of precursor salt, reducing agent, temperature, and solvent type is applied to obtain nanoparticles of the desired morphology. The method enables the fabrication of NPs with high levels of crystallinity and uniform morphology, but process conditions generate high synthesis costs. Higher temperatures are also required in a thermal parsing technique that generates Fe₃O₄ NPs with controlled size. The procedure includes an oxidation process in high boiling temperature organic solvents with stabilizing surfactants (oleic acid, hexadecylamine). However, such magnetite NPs are only dissolved in non-polar solvents. In turn, sol–gel synthesis belongs to wet chemical processes, and it is based on polycondensation and hydrolysis of precursors to form a colloidal sol, and after drying it (removing the solvent), gel, and finally magnetite nanoparticles. The synthesis results in products with high purity and good crystallinity. Additionally, it allows for the production of homogenous structures without using high temperatures. On the other hand, the completion time is relatively high, and the method requires toxic organic solvents. Another method, sonochemical synthesis, applies ultrasound irradiation for the chemical reaction. Ultrasonic bubbles generate high temperatures, pressures, and a strong impact force, promoting multiple reactions. It allows for the formation of small particles with high crystallinity, narrow size distribution, and limited agglomeration. Unfortunately, it is difficult to control the size and shape of the obtained nanoparticles precisely. In turn, the laser ablation method involves using laser power with energies ranging from 90 to 370 mJ. The particle morphology and size distribution can be controlled by using different laser power and organic solvents. Additionally, the ball milling method belongs to physical top-down approaches that generate nanoparticles by breaking up large pieces of the initial material. The particles can be obtained in a ball mill equipped with jars under dry and wet conditions.

Table 1. A collection of the most commonly used methods for obtaining and characterizing magnetite nanoparticles and the main directions of their application.

Fabrication	Coprecipitation Hydrothermal synthesis Thermal parsing Sol–gel synthesis Sonochemical method Laser ablation Ball milling
Characterization	FTIR, NMR SEM, TEM EDX XPS XRD N ₂ adsorption–desorption BET, BJH DLS TGA VSM, SQUID
Application	Biomedical Wastewater treatment Energy Electronics Agriculture Others

Magnetite nanoparticles can be characterized using different physicochemical techniques (Table 1) [6,8]. Fourier transform infrared (FTIR) spectroscopy generally analyzes the chemical structural properties, while solid-state nuclear magnetic resonance (NMR) is much less frequently used. The morphology is investigated using scanning electron (SEM) and transmission electron (TEM) microscopies, while elemental analysis is achieved through energy-dispersive X-ray spectroscopy (EDX). X-ray photoelectron spectroscopy (XPS) is also a technique used to measure the material surface's elemental composition and formation of chemical bonds. X-ray diffraction (XRD) data are used for crystal structure characterization, while textural properties are described based on nitrogen adsorption–desorption isotherm analysis. The Brunauer–Emmett–Teller (BET) method is used to calculate specific surface area, while the Barrett–Joyner–Halenda (BJH) method is used to calculate pore size distribution and pore volume. The hydrodynamic diameter of nanoparticles is measured with the dynamic light scattering (DLS) technique. Moreover, thermogravimetric analysis (TGA) is often applied to evaluate the thermal degradation of the material. Finally, the magnetization of nanoparticles can be verified by using a vibrating sample magnetometer (VSM) or super quantum interference device magnetometer (SQUID).

The global market is increasingly interested in using magnetite nanoparticles in various industrial fields [6]. The main sectors of interest are biomedical and environmental applications. The positive impact of magnetite nanoparticles on the environment could be applied for water treatment using different processes (adsorption, ion exchange, oxidation) or in the catalytic process of alternative energies (biofuels, hydrocarbon cracking) [9]. Other highly developed sectors for the use of magnetite nanoparticles include electronics (data storage, battery electrodes), energy (solar cells, batteries), agriculture (fertilizers, food packaging), and others (e.g., pigments, magnetic ink) [10].

1.1. Magnetite Nanoparticles for Biomedical Application

Although magnetite-based systems are extensively researched as valuable materials in various industrial domains, their biomedical applications represent a significant area of research interest. Nonetheless, the materials must possess particular physical and chemical properties. Therefore, magnetite-based nanoparticles must demonstrate appropriate monodispersity, hydrodynamic diameter, core size, and magnetization. They must also be characterized by good biocompatibility and biodegradability, low toxicity, and water dispersibility. Utilizing a protective coating is a standard method to prevent agglomeration of the magnetite core and enhance its biocompatibility. Biopolymers such as dextran from the polysaccharide group, synthetic polymers like polyethylene glycol, and surfactants are frequently employed. Furthermore, the coating can also consist of an inorganic material, typically silica or carbon. Crucially, it is feasible to introduce reactive functional groups (e.g., amine or carboxyl) onto the surface of the nanosystem for each type of covering, whether organic or inorganic. As a result, diverse active components can be attached to the system based on the intended application. Typical functionalizers of magnetite nanoparticles are antibodies, peptides, genes, selective ligands, aptamers, siRNA, ssDNA, dendrimers, drugs, or fluorophores [11,12]. The nanomaterials based on magnetite nanoparticles are unique systems that can be used in various areas of cancer therapy and diagnostics, including chemotherapy, photothermal therapy, photodynamic therapy, hyperthermia, gene therapy, bioseparation, imaging, tissue engineering, or drug delivery [3,4,7,12,13].

Thermal therapies involve heating target sites (tissue, cells) with an external source. Hyperthermia (HT), an abnormal increase in body temperature, is a natural immune system response during infection. Therefore, HT could be applied as a part of treatment by exposure of body tissue to a temperature range of 40–45 °C [14]. Nevertheless, this could induce adverse effects on adjacent tissues; thus, magnetic hyperthermia (MHT) might present a safer alternative. MHT uses magnetic fields for heat generation and contributes to the destruction of cancer cells (apoptosis or necrosis), which are much more susceptible to high temperatures than healthy cells. Fe₃O₄ NPs act as heating agents when exposed to an alternating magnetic field (AMF). It is a non-invasive method, as the

magnetic field is not absorbed by living tissues, while increasing the temperature of the cancer microenvironment. AMF can penetrate deeply inside different tissues; thus, this method could be adapted for tumor treatment in various positions in the human body. The temperature increase in magnetite nanoparticles under exposure to AMF results from Néel relaxation (reorientation of magnetite NP domain within a particle) or Brownian relaxation (rotation of magnetite NP domain to reverse the direction of the magnetic moment). The clinical application of Fe₃O₄ NPs is analyzed using the specific absorption rate (SAR) that defines the transfer of magnetic energy to thermal energy.

Photothermal therapy (PTT) generates heat for thermal ablation of tumor cells by activation of photothermal agents using laser irradiation in the near-infrared (NIR) region (700–1200 nm) [15,16]. It is also a slightly invasive method that uses thermal energy. PTT therapy destroys cancerous tissues, while it is harmless to healthy tissues. The photothermal agents should be characterized by good biocompatibility, low toxicity, and a high absorption cross-section. The role of a photothermal agent can be fulfilled by magnetite nanoparticles, as well as other components of magnetite-based nanosystems—carbon-based materials (e.g., graphene oxide), nanometals (e.g., Au, Ag), or others (e.g., MoS₂, CoFe₂O₄, phthalocyanines).

Photodynamic therapy (PTD) is a new therapeutic approach based on the light activation of a photosensitizer (PS; e.g., chlorine e6 attached to magnetite core) at the tumor site. The PS is irradiated using an appropriate wavelength. After that, toxic reactive oxygen species (ROS) are generated, which destroys tumor cells. After irradiation, PS is excited from the ground singlet state. The photosensitizer acquires energy through fluorescence or phosphorescence. Thus, the PS directly interacts with an electron/hydrogen-bearing agent, forming peroxides or reactive oxygen species that destroy cancer cells through oxidation. Alternatively, energy is transferred to molecular oxygen, creating highly reactive and toxic singlet oxygen.

The biomedical sector uses different imaging methods, but the most common diagnostic techniques include computed tomography (CT), magnetic particle imaging (MPI), magnetic resonance imaging (MRI), and positron emission tomography (PET). Nevertheless, magnetite nanoparticles are predominantly investigated as elements for MRI. MRI allows for the visualization of anatomical structures, physiological functions, and the molecular composition of tissues. It relies on the absorption and emission of energy within the electromagnetic spectrum's radiofrequency (RF) range. It distinguishes itself from other techniques, such as computed tomography (CT), by providing outstanding soft tissue contrast without harmful ionizing radiation [17]. The contrast in MRI results from variations in signal intensity, influenced by factors such as the concentration of water molecules within the tissue, the relaxation times of water protons, and the mobility of water molecules. The use of contrast agents can further enhance image contrast. Magnetite nanoparticles are extensively studied as potential contrast agents exhibiting enhanced specificity and biocompatibility compared to clinically used gadolinium chelates [18].

Finally, magnetite nanoparticles are significantly researched as components of nanocarriers for gene or drug delivery. We present the underlying assumptions of such systems to gain a deeper understanding of their application in drug delivery systems (DDSs), particularly in targeted DDSs for cancer therapy.

1.2. Assumptions of Targeted Drug Delivery Systems

Drug delivery systems (DDSs) refer to technological platforms that prepare and retain drug molecules in appropriate formats for administration [19,20]. Regardless of the route of administration of the active substance (oral, parenteral, ocular, nasal, or rectal/vaginal), it is successively absorbed, distributed, metabolized, and finally excreted. The absorption to the bloodstream occurs by active or passive transport. The desired course of drug release over time should guarantee a constant drug dose over time (zero-order kinetics model), an initially high dose to reach a constant level (first-order kinetics), or a slow drug release over a long period (sustained release). First-generation DDSs are traditional forms of drug

administration (capsules, tablets, creams, syrups, etc.) with several limitations, including poor absorption and bioavailability, high metabolism, and repeated dosing. Therefore, research has been conducted on controlled DDSs, which allow for the released drug to be maintained at a constant level and, consequently, obtain a therapeutic effect over a long time [21].

Another generation of drug delivery systems is more sophisticated as it is responsible for drug delivery to specific tissues/organs. Thus, targeted DDSs reduce the active substance's dose and reduce side effects on nearby tissues/organs. Targeted drug delivery is accomplished through passive and active targeting. In passive targeting, the transmission into the targeted receptor occurs due to a change in a specific property of the system (pH, temperature, size). On the other hand, active targeting involves modifying the drug carrier with a unit (e.g., antibody, aptamer, peptide) with affinity only for targeted cells. Finally, the most sophisticated DDSs include nanorobots, gene delivery systems, or long-term systems (delivery up to 1 year) [22].

Different mechanisms can be used to control the drug release process. Traditional DDSs are mostly dissolution- or diffusion-controlled systems. Controlled DDSs can be categorized as diffusion, osmosis, and swelling control. Additionally, DDSs constructed of biodegradable polymers demonstrate chemically controlled release due to their degradation in biological processes. However, a crucial element of developing controlled and targeted DDSs was the use of systems sensitive to a specific stimulus—stimuli-responsive DDSs. Such DDSs can be categorized into two primary groups, depending on the type of stimuli—physical or chemical. More advanced DDSs have units sensitive to several stimuli, allowing for better control of a single active agent's (or several active agents') release at the desired target locations.

Physical stimuli-responsive DDSs include systems sensitive to temperature, light, magnetic field, or ultrasound wave. Temperature is the most often applied physical stimulus. Thermo-responsive DDSs contain polymers that behave differently depending on the lower critical solution temperature. The drug loading process occurs below this temperature for soluble and hydrated polymers, while drug release occurs above this temperature due to the polymers' dehydration. On the other hand, stimulation by light requires incorporation into DDSs' photosensitive unit, while magnetic-responsive DDSs contain magnetic nanoparticles (including magnetite NPs) sensitive to an external magnetic field. In turn, ultrasound waves penetrate the tissues deep, and the release process from such DDSs occurs through mechanical effects (via acoustic cavitation) and thermal effects (via acoustic radiation).

The most common chemical stimuli are pH-responsive DDSs. Depending on the desired area of drug release, the carriers contain units (polymers) sensitive to acidic (polybases) or basic (polyacids) pH. In turn, redox-responsive DDSs are decomposed in the desired environment due to the redox reaction. In many cases, such a reaction is generated by the increased concentration of glutathione, often observed in cancer cells, which is the basis for the design of target carriers sensitive to this factor. On the other hand, enzyme-responsive DDSs require a component sensitive to a specific enzyme present in a targeted location.

Nanocarriers constitute a particular group of DDSs, as they allow for reducing the dose of drugs, increasing the therapeutic response, or combining highly targeted with prolonged and sustained release. Typical nanocarriers include nanoparticles, nanospheres, nanocapsules, nanofibers, carbon nanotubes, nanoemulsions, hydrogels, liposomes, exosomes, micelles, or dendrimers. Nanocarriers containing magnetite nanoparticles can also occur in various forms. These nanosystems primarily consist of a magnetite core and organic units/shells, defining their intended application in biomedicine [13]. However, Fe₃O₄ NPs can also be located inside liposomes, micelles, hydrogels, mesoporous silica, or dendrimers [23]. In hydrogels, magnetite NPs and active agents (drugs) are dispersed in polymers. The drug release occurs upon contact with water, but the process can be supported by exposition to alternating magnetic field or NIR laser irradiation. Dendrimers

(e.g., polyamidoamine, PAMAM) with three-dimensional structures are composed of repeating monomers. The structure develops as a tree from the core and contains reactive functional groups at the terminal. On the other hand, micelles with lipophilic core could be used for entrapment of magnetite NPs loaded with hydrophobic drugs. External stimuli (AMF, temperature) force the release of the drug from such systems. In turn, liposomes with a lipid bilayer can be used for the entrapment of drug-loaded Fe_3O_4 NPs. This procedure is applied to eliminate poor drug encapsulation efficiency and thermal disruption of micelles. Additionally, mesoporous silica is also often used to load drugs into its pores. The combination of high efficiency of drug encapsulation in silica with the properties of the magnetic core allows for more effective targeting and control of drug release by external factors.

Targeted delivery mainly applies to drugs used in cancer treatment due to the high toxicity of the active substances to both cancer and healthy cells. However, the clinical use of a given system may be significantly limited by its toxicity [24]. Moreover, poor knowledge of their interactions with cells has primarily contributed to the failure of clinical trials conducted so far with their participation [25].

Each year, scientists provide research results on materials based on magnetite nanoparticles for potential use as drug delivery systems in cancer therapy. Based on the Scopus database, since 2015, the number of original articles in this area has been at least 100 (Figure 1). Upon reviewing the most recent literature reports (2021–2023), it is evident that research areas can be categorized into various subgroups. Much attention is still paid to the design of new nanocarriers; hence, many original papers emphasize synthesis procedures, while research aimed at application in cancer therapy is less advanced. On the other hand, numerous publications describe using magnetite-based systems carrying the active substance in treating a specific cancer. Crucially, many reports highlight multifunctional systems capable of performing functions beyond targeted drug delivery, such as those related to hyperthermia or magnetic resonance imaging.

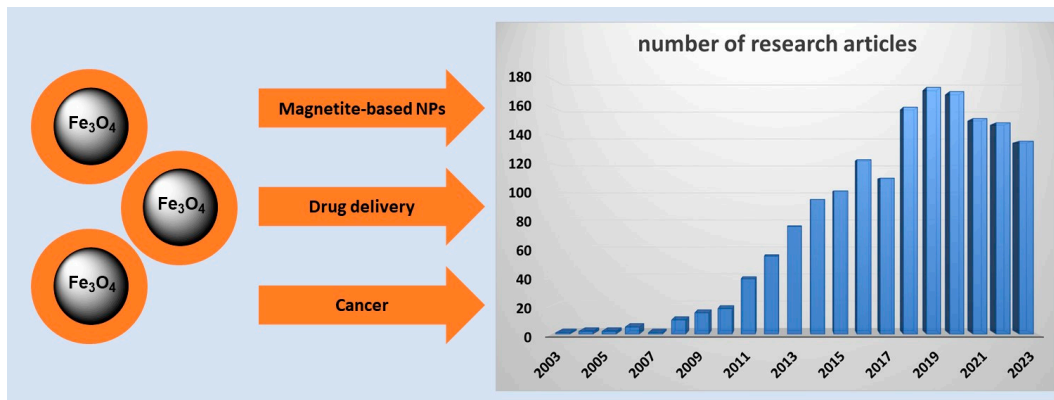


Figure 1. Schematic representation of the number of original research articles (2003–2023) on magnetite-based nanoparticles based on the Scopus database (5 December 2023) using selected terms from the article title, abstract, or keywords.

The current review aims to analyze the latest literature reports from the last three years (2021–2023) regarding possible progress in synthetic procedures and targeting new systems based on magnetite nanoparticles (MNPs) in treating specific cancers. Additionally, the focus is on advancements in employing various techniques to monitor the interactions of these nanocarriers with cells, bringing the potential for their use in clinical trials closer to realization.

2. New Hybrid Systems for Potential Targeted Delivery

Effective drug delivery systems must fulfill specific criteria, encompassing high loading capacity, dispersion stability, and biocompatibility. In order to obtain a material characterized by such properties, Wang et al. [26] proposed a simple solvothermal synthesis of

monodispersed Fe₃O₄ nanospheres with a mesoporous structure and superparamagnetic features. The synthetic route proceeded in the presence of iron chloride, polyvinylpyrrolidone, and urea. The Fe₃O₄ particles with spherical shapes demonstrated almost monodispersive sizes with an average diameter of about 207.3 nm. The material was characterized by the high loading capacity of a model drug—doxorubicin (DOX), 0.36 g/g—attributed to the strong physical adsorption and hydrogen bonding interactions. The *in vitro* cytotoxicity tests demonstrated the neglected effect of the delivery system on cell viability, while only the DOX-loaded nanosphere displayed a cytotoxic effect on selected cancer cells. In continuing these studies, hollow mesoporous Fe₃O₄ nanospheres were acquired without incorporating a template [27]. The hollow structure, mesoporous shell, and rough surface facilitated high DOX loading capacity without using high initial drug concentration. However, drug delivery systems are usually much more complex, and magnetite is only one of the elements.

Polymeric systems, whether natural or synthetic, possess significant potential by enabling a responsive reaction to specific stimuli. This capability facilitates the concentration of nanocarriers at a targeted site. Yoon et al. [28] described a synthesis procedure of magnetic nanocomposites composed of methoxy poly(ethylene glycol), MePEG, grafted to chitosan, to which backbone magnetite nanoparticles and DOX were conjugated. The nanocomposites with spherical shapes demonstrated an average size between 100 and 300 nm. As doxorubicin was attached to the delivery system through disulfide linkage, the drug release was investigated in the presence of glutathione (GSH), responsible for disulfide bond disintegration and occurring at higher levels in cancer cells than in the extracellular environment or normal cells. Therefore, the material demonstrated redox responsiveness and magnetic sensitivity. On the other hand, pH- and thermo-responsive complex nanoparticles were obtained by applying the reverse addition–fragmentation chain transfer (RAFT) polymerization method [29]. Fe₃O₄ nanoparticles were covered with a silica layer and functionalized with amine groups using 3-aminopropyltrimethoxysilane (APS). Then, 4-cyano-4-(phenylcarbonothioylthio)pentanoic acid (CPDB) was attached as a RAFT agent. Subsequently, methacrylic acid (MAA) and *N*-Isopropylacrylamide (NIPAM) monomers polymerized onto the particle surface, and as-prepared PNIPAM-PMMA@Fe₃O₄ was used for DOX loading (Figure 2). An alternative approach was employed to produce a magnetic hydrogel as a carrier for DOX. Poly(acrylic acid/acrylamide) magnetite hydrogel was prepared using radiation synthesis [30].

The hybrid structures with magnetite core could be subjected to various treatments, increasing their potential for targeted delivery of active substances. A compelling concept involves enhancing the drug loading capacity and introducing specific optical properties by decorating magnetite—previously coated with PEG for improved stability—with graphene quantum dots [31]. An alternative suggestion involves incorporating carbon dots (CDs) derived from folic acid. This solution was proposed for a complex DOX support in which Fe₃O₄ was covered with a triazine dendrimer grafted with highly fluorescent CDs [32]. Another approach involved coating the magnetic core with carbon to reduce the non-biocompatibility and toxicity of Fe₃O₄. Subsequently, the material was functionalized with nitric acid and the surfactant Pluronic[®] F-127 to enhance colloidal stability and improve loading affinity for cationic doxorubicin [33]. A higher level of DOX loading was also achieved by MNP stabilization using *N*-(phosphonomethyl)iminodiacetic acid (PMIDA) before silanization [34]. The proposed mechanism assumed simultaneous coordination of DOX on the PMIDA molecule and silanol groups, resulting in a synergistic effect in the drug binding. PMIDA also limited antibiotic desorption, which could be used in drug delivery systems with prolonged action.

The literature also documents the development of magnetic microrobots designed to concurrently deliver multiple drugs, aiming to induce a synergistic effect in cancer therapy. The concept, underpinning the encapsulation of DOX and acetylsalicylic acid (ASA) within a magnetite microrobot, involved utilizing a composition comprising poly(ethylene glycol) diacrylate (PEGDA) and biodegradable gelatin methacryloyl (GelMA) [35]. GelMA, in

combination with PEGDA, was also used to prepare magnetic microrobots with sequential dual-drug release [36]. Gemcitabine (GEM) was conjugated on the surface by a sulfide bond and initially released using near-infrared or a reducing agent (e.g., glutathione, GSH). At the same time, doxorubicin was encapsulated inside and released later during the microrobot decomposition, while magnetite nanoparticles conjugated on the surface through hydrogen bonding were easily separated using weak external stimuli.

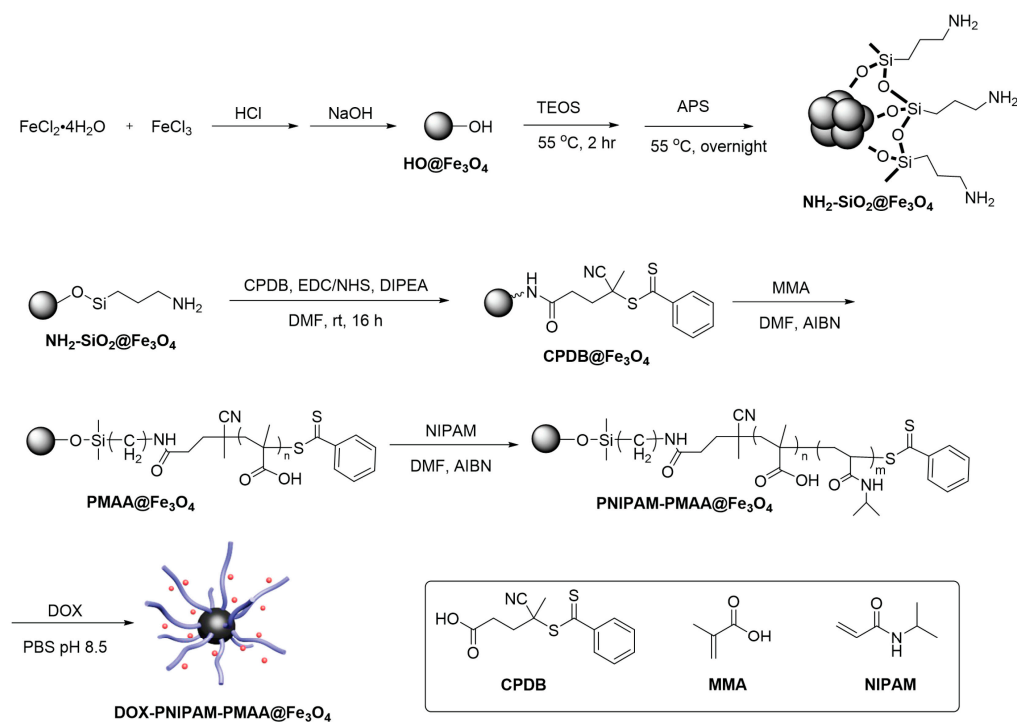


Figure 2. The synthesis procedure of pH- and thermo-responsive magnetic nanoparticles loaded with doxorubicin. Reprinted from [29], *Polymers* (2021).

Literature reports featuring other active substances are less common because DOX predominates as a model anticancer drug. Nevertheless, these reports offer equally valuable solutions for targeted drug delivery. Epirubicin (EPI) is another anthracycline antibiotic, doxorubicin epimer, commonly applied in chemotherapy [37]. It was used as a model agent to evaluate the properties of the nanosystem composed of a magnetite core stabilized with citrate, covered with a silica shell, and decorated with silver nanoparticles [19], demonstrating antibacterial and anticancer efficacy. In the exploration of carriers for other crucial categories of anticancer drugs, there are designs of systems dedicated to antimetabolites, which include methotrexate (MTX) or 5-fluorouracil (5-FU). Functionalized graphene oxide/Fe₃O₄ nanocomposite was proposed as a nanocarrier of MTX [38]. The superparamagnetic graphene oxide demonstrated high water solubility, and MTX delivery was improved by using cyanuric chloride as a crosslinking unit. An alternative suggestion was outlined for delivering 5-FU, involving grafting dimethylaminoethyl methacrylate onto κ-carrageenan. Subsequently, this copolymer was coated onto magnetite using a microwave-supported coprecipitation method [39]. On the other hand, the molecularly imprinted polymer was a strategy for targeted delivery of docetaxel (DTX)—one of the microtubule-damaging agents [40]. The diverse synthetic solutions proposed recently for targeted anticancer drug delivery using magnetite-based nanosystems, along with information on the method of magnetite synthesis and techniques for characterizing the final product, are collected in Table 2.

Table 2. Diverse synthetic solutions for potential optimization of targeted drug delivery using magnetite nanoparticle-based systems in cancer therapy.

Components of Magnetite-Based Delivery System	Fabrication/ Characterization	Loaded Drug	Responsiveness *	Reference
Methoxy poly(ethylene glycol) Chitosan	Commercial product/ NMR, TEM	DOX	Redox-responsive	[28]
Poly (methacrylic acid) Poly (<i>N</i> -Isopropylacrylamide)	Coprecipitation/ FTIR, TGA, SEM, DLS, zeta potential	DOX	pH-responsive Thermo-responsive	[29]
Poly (acrylic acid/acrylamide)	Coprecipitation/ FTIR, XRD, TEM	DOX	pH-responsive	[30]
Polyethylene glycol Graphene quantum dots	Coprecipitation/ FTIR, XRD, TEM, VSM, DLS, TGA, BET	DOX	pH-responsive	[31]
Triazine dendrimer Folic acid-derived quantum dots	Coprecipitation/ FTIR, XRD, SEM, EDX, VSM, N ₂ adsorption–desorption, BET, BJH, zeta potential	DOX	pH-responsive photoluminescent activity	[32]
Carbon Pluronic® F-127	Solution combustion/ FTIR, XRD, TGA, N ₂ adsorption–desorption, BET, SEM, TEM, EDX, DLS	DOX	pH-responsive	[33]
N- (phosphonomethyl)iminodiacetic acid Silica	Coprecipitation/FTIR, TEM, EDX, VSM, zeta potential	DOX	Not available	[34]
Poly(ethylene glycol) diacrylate gelatin methacryloyl	Commercial product/ SEM, EDX, XPS, VSM	DOX GEM	Redox-responsive Thermo-responsive	[36]
Silica Silver nanoparticles	Coprecipitation/ FTIR, XRD, TEM, EDX, TGA, N ₂ adsorption–desorption	EPI	Not available	[41]
Graphene oxide Cyanuric chloride	Coprecipitation/ FTIR, TEM, XRD, XPS, AFM	MTX	pH-responsive	[38]
Dimethylaminoethyl methacrylate κ-carrageenan	Microwave-induced coprecipitation/FTIR, XRD, TEM, VSM, DLS	5-FU	pH-responsive Thermo-responsive	[39]
Molecularly imprinted polymer Fluorescence	Coprecipitation/FTIR, XRD, SEM, EDX, VSM	DTX	Not available	[40]

* Each drug delivery system demonstrates magnetic responsiveness.

3. Magnetite-Based Nanomaterials for Specific Cancer Treatment

Cancer stands as a significant global health challenge. Consequently, it is unsurprising that the quest for efficient carriers for highly toxic anticancer drugs tailored for targeted therapy garners substantial interest within the scientific community. However, the application of magnetite nanoparticles in cancer therapy is strongly affected by numerous factors that must be met—control of size, shape, and composition; toxicity; biocompatibility; and high delivery efficiency to the targeted tumor environment. The primary challenge currently impeding the translation of systems studied in research laboratories to clinical applications is presumably the limited efficiency in delivering nanocarriers to the targeted tumor area. The external magnetic field should control the movement of the nanocarrier but is limited by low tissue penetration.

Despite the range of different cancers, particular attention is focused on materials for potential use in breast cancer therapy. This particular cancer type contributes to the highest number of new cases, although the diagnoses of prostate and lung cancer also remain notably high [42,43]. Therefore, assessing the research progress dedicated to utilizing a specific carrier to treat a particular cancer type is worthwhile. Further analysis of recent research aims to determine whether the methodology for developing a potentially optimal carrier for targeted delivery aligns with advanced investigations into such a drug formulation for cancer therapy. It is assumed that magnetite NPs, deposited on the surface of the targeted cell membrane, are uptaken by cells (through endocytosis), and then the active substance is released intracellularly under the influence of a specific stimulus (e.g., pH). However, at the moment, knowledge about these intracellular interactions is limited.

3.1. Breast Cancer Treatment

The statistics presented by the World Health Organization, indicating a 1-in-8–10 risk of women developing breast cancer, are alarming. However, they also serve as a stimulus for intensive research in this field [42]. The list of selected and recently described targeted drug delivery systems based on Fe_3O_4 NPs for potential application in breast cancer treatment is collected in Table 3. Much like the previously examined original studies, the primary active molecule in systems designed for potential breast cancer therapy is the anthracycline antibiotic—doxorubicin [44]. DOX has a broad spectrum of action but also has several undesirable effects: development of dose-dependent, cumulative, irreversible, and long-lasting cardiotoxic side effects [45].

An interesting proposal for a biocompatible nanocarrier dedicated to the delivery of DOX to breast cancer cell lines was presented by Ehsanimehr et al. (Figure 3) [46]. Fe_3O_4 nanoparticles were initially coated with a silica layer using tetraethyl orthosilicate (TEOS) and modified with mesoporous silica SBA-15. Mesoporous silica with a high surface area should enhance loading efficiency and protect a drug. It is also capable of surface functionalization. In the next step, functional groups were introduced on the surface via trimethoxy vinyl silane (TMVS), which was used to modify the surface with the amino acid L-cysteine. At the same time, polyethyleneimine (PEI)—a branched polymer capable of DNA complexing—was modified by carboxymethyl- β -cyclodextrin (CM- β -CD) for the elimination of undesired reactions between PEI and serum components and for embedding folic acid (FA) into the CD cavity. FA should increase targeting to folate receptors that are overexpressed in many cancerous cells. Finally, PEI/CM- β -CD/FA was grafted onto mesoporous material. The pH-responsive core-shell nanocarrier demonstrated initial burst release due to the partial location of DOX molecules at the surface of the polymeric network. Faster DOX release was observed in an acidic environment due to repulsion between the drug molecules and the nanocarrier and partial destruction of hydrogel bonds that facilitated the drug release. The *in vitro* MCF-7 breast cancer cell viability assay showed that the half-maximum inhibitory concentration (IC_{50}) was 0.511 $\mu\text{g}/\text{mL}$ and 0.23 $\mu\text{g}/\text{mL}$ for free DOX and DOX loaded in the nanocarrier. Hence, the utilization of the carrier results in lower cancer cell survival and a reduced dosage of DOX. The fluorescence microscopy imaging showed that the cellular uptake process was completed in 3 h. It also showed that only DOX-loaded nanocarrier induced chromatin fragmentation, while the nanosystem itself did not influence the morphology of breast cancer cells. Moreover, the fragmentation was more significant than for free DOX. Additionally, the nanocarrier was considered biocompatible because only a small, negligible hemolytic effect was observed for high dosage.

The silica-coated magnetite nanoparticles ($\text{Fe}_3\text{O}_4@\text{SiO}_2$) also served as the initial material for the nanocarrier, which was then modified with tragacanth gum derivative—a natural anionic polysaccharide characterized by a multibranched structure—and folic acid as a targeting agent [47]. Coating of magnetite nanoparticles with carboxymethyl tragacanth ensures a hydrophilic surface that protects against agglomeration, increases the dispersion of nanoparticles, and improves bioavailability. The protonation of carboxylic groups in

The *in vitro* DOX release was investigated under acidic and reduction conditions. In acidic media, the hydrogel shrank, while in glutathione (GSH; overproduced in many cancerous cells) solution, disulfide bonds in cystamine were reduced, resulting in increased DOX release. The hydrogel could strongly interact with human serum albumin (HSA) due to the high affinity of hydrogel biomaterials to HAS protein. As a consequence of protein-biomaterial interactions, characteristics of biomolecules undergo significant modifications. Therefore, the fluorescence emission intensity of HSA decreased with increasing hydrogel concentration. Thus, the nanocarrier acted as a quencher via a dynamic mechanism and probably caused structural changes in HSA (unfolding of protein structure on the hydrogel surface).

On the other hand, a derivative of another polysaccharide, carboxymethyl chitosan, combined with a derivative of aromatic natural polymer-aminated lignosulfonate was used to fabricate pH-responsive nanoparticles with uniform size [49]. Lignin with a polyphenol structure contains many reactive functional groups; thus, it can be easily modified. It is also biocompatible and biodegradable, demonstrating antioxidant, antibacterial, and anti-inflammatory properties. On the other hand, chitosan—a cationic polysaccharide—demonstrates pH responsiveness and improves drug internalization into cells. Two modified polymers were immobilized on a magnetite core. Aminated lignosulfonate resulted in electrostatic repulsion and steric hindrance between the magnetite-based NPs, protecting them against aggregation. MTT assay and live/dead staining experiments proved that a DOX-loaded nanocarrier inhibited cancer cell growth, and cell viability decreased with increasing concentrations of the drug-loaded delivery system.

Besides natural polymers, synthetic polymer units have also been introduced in recently published original papers. $\text{Fe}_3\text{O}_4@SiO_2$ nanoparticles were subjected to coating with DOX-imprinted poly(methacrylic acid-*co*-diallyl dimethylammonium chloride) to form a cationic magnetic nanocomposite [50]. Commonly, cancer cells are characterized by a negative charge; thus, a positively charged nanocarrier should penetrate such cells more efficiently. Importantly, molecularly imprinted polymer synthesized with a template molecule (DOX) guarantees high drug loading efficiency. Histopathological analysis showed the system's effectiveness in preventing tumor cell proliferation and increasing apoptosis while maintaining a limited influence on other tissues.

On the other hand, poly(*N*-isopropyl acrylamide) (PNIPAM) was used for the fabrication of a thermosensitive magnetic nanocarrier [51]. PNIPAM undergoes transitions in response to temperature (LCST 32–34 °C). PNIPAM chains are water soluble below the LCST, collapse around the LCST, and above the LCSTs, the interactions between chains and water molecules destroy hydrogen bonds. Therefore, the DOX release was analyzed at 30 (below), 34 (around), and 38 (above) °C. The highest cumulative release was observed at 30 °C due to physical interactions between polymer chains and water molecules. The DOX-loaded nanosystem displayed high activity over MCF-7 breast cancer cells and cytoskeleton organization, while the pristine nanocarrier had good biocompatibility. Another example of an absorbing carrier was designed using non-ionic polymers—polyvinyl alcohol (PVA) and polyvinylpyrrolidone (PVP)—and two ligands to actively target breast cancer cells— β -estradiol for estrogen receptors and folic acid for folate receptors [52]. The selected ligands belong to the best-known breast cancer biomarkers. The polymers PVA and PVP were selected due to their widespread use in numerous pharmaceutical applications and non-ionic nature. The ligands showed a tumor-targeting effect and enhanced drug uptake but also stabilized nanoparticles.

Alternative approaches suggested in recent scientific papers rely on drug delivery systems that are considerably simpler. An illustration is a nanocomposite composed of a magnetic core and CaCO_3 , which exhibited promising properties in effectively inhibiting MCF-7 cell lines [53]. The oleic acid-modified magnetite core was coated with porous CaCO_3 using the coprecipitation method. The material demonstrated high loading efficiency (1900 μg DOX/mg) and stability at physiological pH, while demonstrating efficient DOX release in acidic media. The experiments with human serum albumin solution indi-

cated that the drug release was promoted by forming a protein corona—a protein coating on the surface of nanomaterials in biological fluids that improves biodistribution, biocompatibility, or cellular interactions. On the other hand, magnetite nanoparticles covered with citric acid (CA) were proposed as a potential DOX delivery system in the treatment of triple-negative breast cancer—an uncommon breast cancer subtype without an identified molecular target [54]. Citric acid is a popular surfactant, with one hydroxyl and three carboxyl functional groups, that stabilizes magnetite nanoparticles in aqueous suspensions. The *in vitro* studies were carried out using the 4T1 breast cancer cell line to study the metastatic nature of the cancer and the MDA-MB-468 breast cancer cell line characterized by lack of expression of estrogen, progesterone, and human epidermal growth factor receptors. In optimized formulations, the DOX-loaded nanosystem showed a synergistic effect on the cell cultures compared to pristine doxorubicin. The proposed mechanism is demonstrated in Figure 4. In brief, the nanoparticles are responsible for forming the reactive oxygen species that catalyze the Fenton reaction. At the same time, active oxygen species are formed during drug-induced apoptosis. The synergism results in better penetration and improved drug uptake. Additionally, active oxygen forms could be responsible for cell DNA damage.

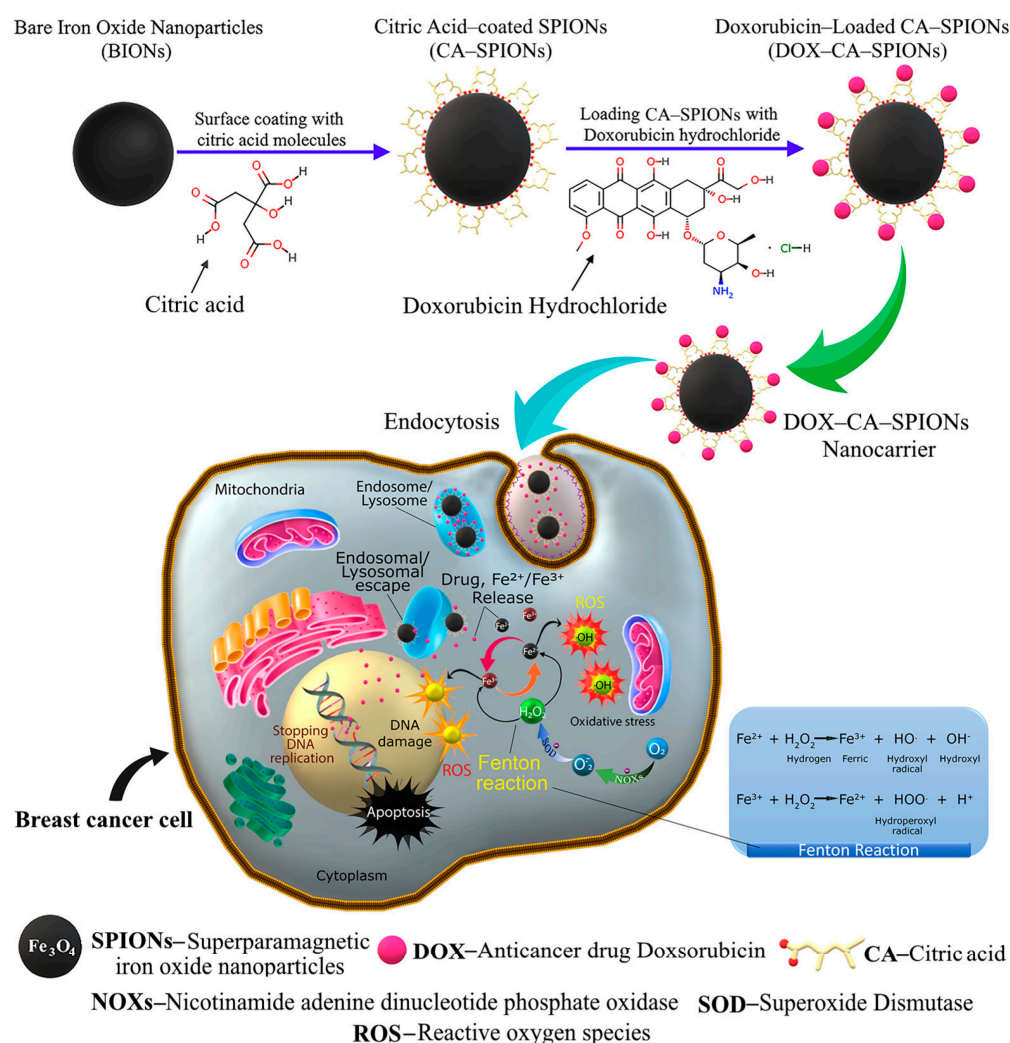


Figure 4. Proposed anticancer mechanism of the DOX-loaded citric acid coated-magnetite nanoparticles. Reprinted from [54], *Pharmaceutics* (2023).

A distinctly different approach was suggested for a magnetic carrier prepared utilizing a natural porous silica structure, namely, diatoms [55]. Diatoms are algae characterized by biosilica with high mechanical stability and high surface area, biocompatibility, and

thermal and chemical resistance. Thus, the material is suitable for controlled drug delivery. A magnetic microrobot was fabricated using *Thalassiosira weissflogii* frustules as a biological template, followed by magnetite NPs adhering to the frustules' surfaces through electrostatic adsorption. In general, magnetic nano/microrobots are fabricated using synthetic materials (expensive), living cells (difficulties in maintaining cell viability), and natural biological templates. The latter combines the beneficial features of high biocompatibility with the desired structural properties and can be combined with other components. The operation of micro/nanorobots is based on the ability to convert energy into motion, hence the growing interest in this group of systems, especially as the most sophisticated DDSs [56–58]. The diatom-based biohybrid microrobot demonstrated high DOX-loading capacity and pH sensitivity. Notably, the possibility of magnetic control of the nanocarrier was deeply investigated. The microrobots can be controlled individually and as dimers, trimers, or multimers. However, high drug delivery efficiency is possible only by using swarms of microrobots. Low concentration of the biohybrid microrobots resulted in independent movements due to long distances between magnetic species. On the other hand, higher concentrations initiated the interaction, followed by the swarming behavior and, consequently, larger-dose drug delivery.

Lately, several original papers have emerged featuring other drugs loaded into magnetite-based nanocarriers for the potential treatment of breast cancer. Platinum-based drugs (e.g., cis-platin, cis-[Pt(NH₃)₂Cl₂]) are responsible for the direct damaging of DNA and are used for the treatment of various cancers. Carboplatin functions as an alkylating agent that produces platinum complexes. The complexes are linked to the DNA, resulting in double-strand breaks. Magnetite–chitosan (CS-Fe₃O₄) and magnetite–chitosan–graphene oxide (CS-Fe₃O₄-GO) nanocomposites were used for loading and targeted delivery of carboplatin to breast cancer cell lines [59]. The entrapment of the drug in magnetite-based systems reduced the systemic toxicity of carboplatin and enhanced its activity against MCF-7 cell lines. However, the release rates in the physiological and acidic medium were only slightly different. On the other hand, platinum could also be applied as a nanoenzyme with catalytic activity responsible for directly combating cancer cells and subsequently improving drug permeability. Therefore, the Fe₃O₄ nanospheres loaded with platinum and 5-fluorouracil and coated with polyethylene glycol (Fe₃O₄/Pt-5-FU@PEG) were investigated as platforms for the treatment of solid breast cancer [60]. The nanocarrier showed pH-sensitive drug release under acidic conditions. Pt demonstrated peroxidase and catalase mimic activity, increasing levels of reactive oxygen species and O₂. Cytotoxicity studies proved reduced proliferation of 4T1 cancer cells, while in vivo studies showed tumor size reduction and overcoming its hypoxia. Platinum was also introduced into core–shell nanospheres composed of an Fe₃O₄-Pt@metal–organic framework (MOF) for epirubicin delivery [61]. The nanocarrier was synthesized by hydrothermal and layer-by-layer methods. MOF coating should increase porosity, colloidal stability, bioavailability, catalytic activity and facilitate drug release in an acidic environment. The nanoplatform exhibited pH-sensitive drug release in a tumor microenvironment. EPI-loaded nanospheres effectively inhibited triple-negative 4T1 cancer cell proliferation due to improved penetration compared to pristine EPI. However, the in vitro results were not confirmed by in vivo studies. MOF was also successfully adapted to prepare the targeted delivery system of antibiotic ciprofloxacin (CPX) [62]. MOFs produced from transition metal ions are biocompatible, chemically stable, capable of modification, and have high drug loading efficiency. In turn, a particular group of MOFs, Material Institute Lavoisiers (MILs), are a network of trivalent ions and carboxylic acid-derived linkers. Therefore, MIL-100(Fe) with high surface area and stability was applied for drug encapsulation. MIL-100(Fe) was prepared in the presence of magnetite–silica NPs. The nanomaterial demonstrated the biocompatibility, while the CPX-loaded nanocarrier showed significant toxicity against cancer cells.

Among the systems designed for delivering alternative drugs, it is noteworthy to mention the system incorporating an aptamer (Apt) conjugated to paclitaxel (Fe₃O₄@PTX-Apt) [63]. The aptamer is a peptide or oligonucleotide molecule acting as a chemical

antibody. Epithelial cell adhesion molecule (EpCAM) is overexpressed in many human cancer cells; thus, it was chosen as a specific DNA aptamer. Magnetite nanoparticles were covered with gold and cysteamine. Subsequently, PTX was modified to introduce carboxyl groups and disulfide bonds (PTX-S-S-COOH) and finally reacted with amine groups of cysteamine. Additionally, thiol-modified aptamer was also conjugated to the magnetic nanocarrier. Specific aptamer molecules facilitated drug delivery into EpCAM-positive cells, enhancing cytotoxicity against MCF 7 and 4T1 cancer cells, while limiting toxicity to reference normal breast cell line MCF-10A without EpCAM. Flow cytometry studies confirmed that the nanocarrier with the aptamer did not enter MCF-10A cells; thus, internalization of Fe_3O_4 @PTX-Apt in EpCAM positive cells was significantly higher compared to reference Fe_3O_4 @PTX.

The breast cancer MCF 7 cell lines were also used to investigate magnetite nanoparticles functionalized with L-cysteine and hyaluronic acid loaded with tamoxifen (TMX)—a drug belonging to the selective estrogen receptor modulators [64]. Hyaluronic acid is often selected due to its high affinity towards the cluster determinant 44 (CD 44) receptor, overexpressed on the surface of many cancer cells, while the presence of amino acids improves colloidal stability. The increased cytotoxicity of the TMX loaded in the nanocarrier against the breast cancer cells yielded an equivalent anticancer activity compared to free TMX, but at a concentration four times lower. Significantly, L-cysteine influenced enhanced anticancer activity.

Some literature reports combine the design of new targeted carriers of active substances and the use of compounds of natural origin, mainly polyphenols (e.g., curcumin, quercetin), as potential agents with anticancer properties. An illustration is a complex system comprising a magnetic core designed to co-deliver hydrophilic doxorubicin and hydrophobic curcumin (CUR), Figure 5 [65]. Initially, magnetite- β -cyclodextrin (Fe_3O_4 - β -CD) nanocomposite was formed and covered with 3-aminopropyltrimethoxysilane to introduce amine functional groups. The triazine dendrimer (TD) shell was subsequently created in the presence of citric acid and melamine. The process of dendrimer growth was carried out until generation 2.5 was obtained (Fe_3O_4 - β -CD-CTD G2.5). After that, carboxylic groups of Fe_3O_4 - β -CD-CTD G2.5 reacted with amine groups of folic acid to create Fe_3O_4 - β -CD-CTD-FA. The presence of cyclodextrin cavities and the branched dendrimer structure assured the high loading capacity of both active molecules. The nanocarrier demonstrated high antioxidant activity and biocompatibility against MDA-MB-231 breast cancer cells. The presence of folic acid (folate receptor-mediated endocytosis) and curcumin improved the DOX cellular uptake by breast cancer cells, increasing topoisomerase II-mediated DNA cleavage in the cytoplasm.

Curcumin was also successfully encapsulated in magnetic nanoparticles to co-deliver two active agents with different polarities—CUR and piperine (PIP) [66]. PIP molecules were attached to the chitosan surface, while CUR molecules were entrapped into the zein matrix. The polymeric carrier with magnetite core was coated with chitosan to create a CUR-PIP-loaded polymer magnetic system demonstrating significant synergistic cytotoxicity against MCF 7 cells. The nanoprecipitation approach increased the bioavailability of CUR and PIP, resulting in increased toxicity to cancerous cells compared to free forms of active agents.

On the other hand, a magnetite–graphene quantum dots hybrid with conjugated folic acid was investigated as a curcumin delivery system to enhance the potential drug efficiency in cancer treatment [67]. The hybridization of magnetite NPs with graphene quantum dots (GQDs) should improve the properties of the composite material. GQDs are highly soluble, biocompatible, demonstrate high loading capacity and photoluminescence activity. The cancerous cell viability was reduced with increasing CUR concentration (until 80 $\mu\text{g}/\text{mL}$) and decreased to 2%, but the cytotoxic effect was more efficient for MCF-7 than for MG-63 cells.

In another approach, graphene oxide functionalized with polyvinylpyrrolidone (PVP) was used as a cover of magnetite to efficiently encapsulate quercetin (QR) via noncovalent

interactions and consequently increase its effectiveness against breast cancer cells [68]. Graphene oxide demonstrates a strong ability to load organic molecules through hydrogen bonding, electrostatic, or π - π interactions, while PVP ensures biocompatibility and hydrophilicity. Therefore, the QUR-loaded nanocarrier demonstrated improved toxicity against MDA-MB 231 breast cancer cells compared to the free active agent.

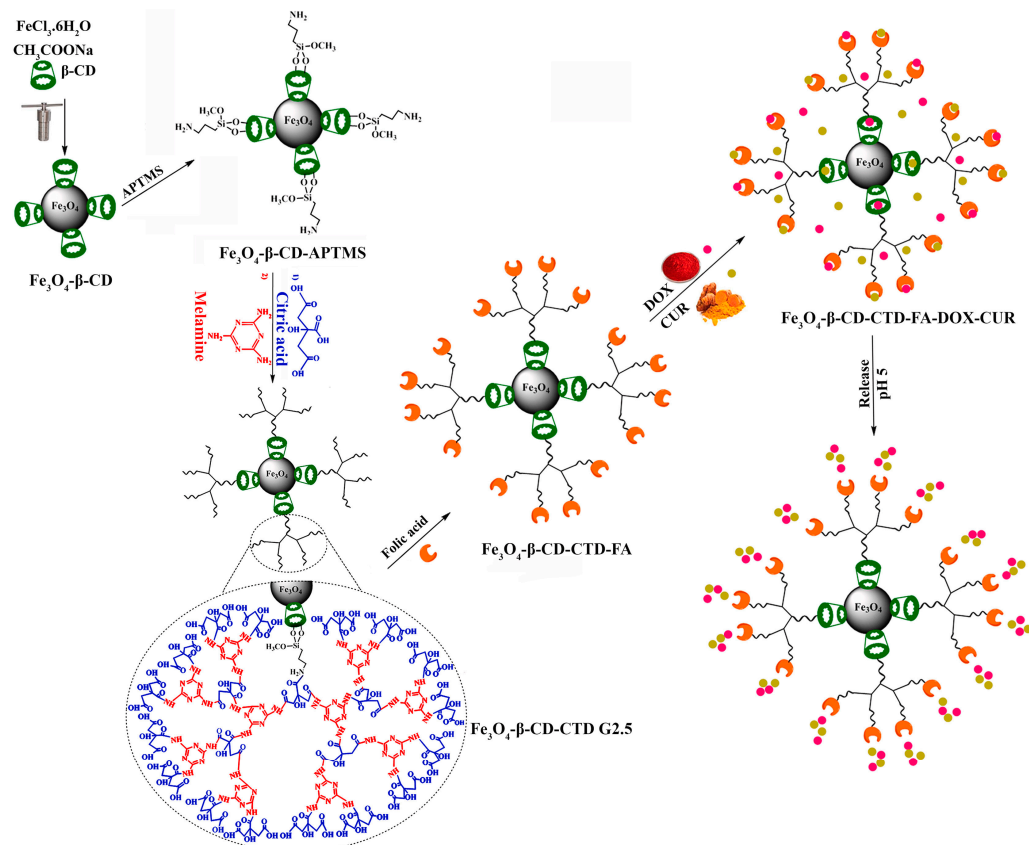


Figure 5. Schematic representation of synthesis procedure of Fe_3O_4 - β -CD-CTD-FA for co-delivery of DOX and CUR. Reprinted from [65], Copyright (2023), with permission from Elsevier.

Table 3. Recently described targeted drug delivery systems based on Fe_3O_4 NPs for potential application in breast cancer treatment.

Components of Magnetite-Based Delivery System	Cell Model	Characterization of Anticancer Properties	Reference
SBA-15, L-cysteine, PEI, CD, FA	MCF7	Drug release, cell viability, cellular uptake, biocompatibility	[46]
Tragacanth gum, FA	MCF7	Drug release, cytotoxicity, cellular uptake	[47]
Oxidized alginate, cystamine	MCF7	Interaction with human serum albumin, cytocompatibility, cytotoxicity	[48]
Carboxymethyl chitosan, aminated liginosulfonate	MCF7	Drug release, cytotoxicity	[49]
Cationic molecularly imprinted polymer	4T1	Drug release, cytotoxicity, hemolysis assay In vivo: tumor induction, tumor volume, histopathological studies	[50]

Table 3. Cont.

Components of Magnetite-Based Delivery System	Cell Model	Characterization of Anticancer Properties	Reference
poly(<i>N</i> -isopropyl acrylamide)	MCF7	Drug release, biocompatibility, cell viability, cellular uptake	[51]
Polyvinyl alcohol, polyvinylpyrrolidone, FA, β -estradiol	MCF7	Drug release, cell viability, cytotoxicity	[52]
CaCO ₃	MCF7	Drug release, cytotoxicity	[53]
Citric acid	4T1 MDA MB 468	Drug release, cytotoxicity	[54]
Diatoms	MCF7	Drug release, biocompatibility, cytotoxicity	[55]
Chitosan, graphene oxide	MCF7	Drug release, cytotoxicity	[59]
Polyethylene glycol	4T1	Drug release, enzyme-mimic activity, cell viability, apoptosis In vivo: tumor condition	[60]
Metal–organic framework	4T1	Drug release, cytotoxicity	[61]
Silica, metal–organic framework	MCF7	Drug release, cytotoxicity	[62]
Au, cysteamine, aptamer	4T1 MCF7	Drug release, cytotoxicity	[63]
Hyaluronic acid, L-cysteine	MCF7	Drug release, cytotoxicity	[64]
β -cyclodextrin, glycodendrimer, FA	MDA MB 231	Drug release, cytotoxicity, cellular uptake, antioxidant activity	[65]
Chitosan, zein	MCF7	Drug release, cytotoxicity, synergistic effect	[66]
Graphene quantum dots, FA	MCF7 MG63	Drug release, cytotoxicity	[67]
Polyvinylpyrrolidone, graphene oxide	MDA MB 231	Drug release, cytotoxicity	[68]

3.2. Treatment of Other Cancers

While systems primarily designed for potential breast cancer treatment dominate, many original papers elucidate magnetite-based systems for targeted drug delivery to other types of cancers. Consequently, further discussions on recently presented systems will be categorized based on their potential application against specific types of cancer cells (Table 4).

Primary liver cancer refers to a disease in which cancer cells arise in the liver, and its most common type is hepatocellular carcinoma. Despite well-characterized risk factors of liver cancer (chronic infection with hepatitis B virus (HBV) or hepatitis C virus (HCV), heavy alcohol consumption, metabolic diseases, and aflatoxin exposure), it contributes to one of the highest mortality rates worldwide among deaths caused by cancer [69]. Therefore, systems that limit the toxic impact of the carried active substance on healthy cells and its targeted delivery to the areas with cancerous tissue are also the subject of intensive research.

Wang et al. [70] used polysaccharide dextran (DEX) and polylactic acid (PLA) for covering magnetite nanoparticles and DOX loading and subsequently applied them for the study of liver cancer inhibition. The animal experiments showed that tumor weight decreased approximately twice when using a DOX-loaded nanocarrier compared to free DOX, indicating a more substantial inhibitory effect on liver cancer cells. Additionally, the survival time also increased to 63 days, while for free DOX-treated animals, it was only 36 days. In another approach, Fe₃O₄ nanoparticles were coated with Pluronic F127

crosslinked with polyethyleneimine to create a pH- and thermo-responsive nanocarrier of doxorubicin [71]. Pluronic F127 is an amphiphilic polymer that improves solubility and drug encapsulation. It is stimuli-responsive (pH, temperature) and can load hydrophilic and hydrophobic drugs. Branched cationic polyethyleneimine (PEI) can conjugate to DNA/RNA, causing osmotic imbalance and increasing cellular uptake due to attraction interactions with negatively charged phospholipids/glycoproteins at the cellular surface. The human hepatocellular carcinoma (HepG2) cells incubated with the DOX-loaded carrier demonstrated higher doxorubicin uptake than those incubated with pure DOX using analogous concentration. It was also suggested that the endocytosis pathways in endothelial and epithelial cells affect the interactions between the DOX-loaded nanocarrier and cells upon alternating magnetic field.

In turn, the combination of magnetite and boron nitride was used to potentially increase the synergistic chemodynamic, photodynamic, and immune therapy [72]. Boron nitride nanosheet (“white graphene”) demonstrates low toxicity, capability of chemical bond formation, biocompatibility, and biodegradability. Additionally, PEG, synthesized via benzoic imine, was introduced onto the nanocomposite surface to stabilize DOX release towards cancer cells and pH-responsiveness. The *in vivo* tests showed that the application of the DOX-loaded nanocarrier resulted in more significant tumor inhibition than pure DOX. The liver cellular uptake studies showed the influence of the DOX-loaded nanocarrier on cell morphology. It was suggested that improved cellular drug uptake resulted from the DOX-loaded carrier bypassing the P-glycoprotein efflux system in cancer cells, which helped to eliminate drug resistance. Thus, the mandatory factor affecting nanocarrier–cell interactions is again endocytosis pathways in endothelial/epithelial cells. The histopathological studies indicated nuclear shrinkage and cytoplasmic leakage of liver tumors, while no pathological changes were observed in other organs.

In the original paper of Wang et al. [73], another organic unit was used to modify the magnetite surface—deoxycholic acid derivative combined with folic acid. Cholic acid and its derivatives should improve the stability of drug metabolism and confer selectivity towards the liver. Therefore, magnetite initially functionalized with amine functional groups participated in a reaction with formyl deoxycholic acid (FDCA) and folic acid (FA) to obtain an FDCA-FA-Fe₃O₄ nanocarrier of doxorubicin. The material studied demonstrated excellent blood compatibility in a specific concentration range, thus ensuring safe DOX delivery in the blood. Importantly, cellular uptake studies showed selectivity of the nanocarrier towards hepatoma cells due to the presence of FDCA, while FA was responsible for cancer cell targeting. Moreover, apoptosis staining proved a low concentration of DOX-loaded nanocarrier in viable cells while being strong in apoptotic cells. It is also significant that the drug carrier selectively targeted hepatocellular carcinoma cells (HepG2) compared to esophageal carcinoma cells (K150). Additionally, Western blotting was applied to analyze the expression of caspase-3 protein, necessary in the early stage of apoptosis, in HepG2 cells. The experiments confirmed the influence of DOX-loaded nanocarrier on increasing caspase-3 expression. Another solution for targeted DOX delivery to the HepG2 cells was based on a system composed of magnetite nanoparticles and Zn-Al layered double hydroxides (Zn-Al LDHs) [74]. Zn-Al LDH nanosheets should protect magnetite against aggregation and assure uniform decoration, while Fe₃O₄ nanoparticles should stabilize the composite structure and prevent restacking of the nanosheets. The nanocarrier demonstrated high loading efficiency (0.23 g/g) and a pH-responsive release profile. The DOX-loaded Fe₃O₄/Zn-Al LDH nanocarrier showed a significant inhibition effect on the proliferation of HepG2 liver cancer cells. The drug-free nanocarrier had no significant influence on cell morphology, confirming good biocompatibility, while the presence of the DOX-loaded carrier resulted in an apoptotic effect that increased with increasing drug concentration.

Literature reports also encompass alternative active compounds within delivery systems targeting liver cancer cells. Sorafenib (SFB) inhibits the formation of nucleic acids by connecting to DNA. Simple, PEG-coated magnetite nanoparticles were used for SFB loading and characterized for potential application in liver cancer treatment [75]. The presence of

PEG was beneficial for better stability, biocompatibility, lower toxic and pharmacokinetic effects. The incorporation of SFB in the nanocarrier improved its anticancer activity towards HepG2 cancer cells. Analogous components in different formulations were used to fabricate PEG-modified nanoparticles to co-encapsulate magnetite nanoparticles and SFB [76]. Magnetite NPs and SFB were loaded into PEG solid lipid nanoparticles prepared using an oil-in-water homogenization process. The anticancer activity of the SFB-loaded NPs was more effective than free SFB after exceeding 48 h of cell incubation. Importantly, under-skin micromagnets were implanted (in vivo) above the liver to ensure SFB accumulation in liver cancer cells. The impact of magnetic field topographies was evaluated using two different magnet configurations—joined magnets and two magnets separated by a Teflon spacer. Two-dimensional simulation analysis and in vivo studies with sleeping mice placed on the XYZ-3-axis micropositioner stage showed higher attractive forces acting on the magnetic nanoparticles when two magnets were separated (higher magnetic field gradient). Consequently, this topography ensured the highest targeting efficacy and showed the importance of this parameter on the magnetic targeting performance.

In other reports, zinc–aluminum layered double hydroxide (Zn–Al LDH) and polyvinyl alcohol were used to coat Fe_3O_4 and, subsequently, to deliver 5-FU to HepG2 cancer cells [77]. The designed formulation was non-toxic and biocompatible with normal cells, while it showed more effective anticancer activity (dose-dependent) than free DOX. In turn, another active substance appears in studies based on PEGylated magnetite nanoparticles—crocetin (CRT) [78]. *Crocus sativus* L. (saffron) contains several biologically active components, including CRT, a dicarboxylic acid precursor of crocin (mono- and di-glycosyl polyene ester). Crocetin was chemically bonded to PEGylated Fe_3O_4 and demonstrated potential for reducing HepG2 cell proliferation. It was suggested that the CRT-loaded nanocarrier should primarily be located in cancer tissue by passive targeting. Subsequently, degradation of PEG coating and magnetite NPs followed by free iron ions binding to ferritin proteins would result in the release of CRT. On the other hand, Au and PEGylated Fe_3O_4 nanoparticles were tagged with two monoclonal antibodies (mAbs) for hepatocellular carcinoma-targeted therapy [79]. Avastin (AVS), mAbs against vascular endothelial growth factor, was linked to the PEGylated magnetite, while gold was tagged with mAb against cancer stem cell marker (CD90). The histopathological studies proved the best improvement in liver architecture and regression of tumors after using the system with two monoclonal antibodies compared to the one that included only AVS or nonconjugated Fe_3O_4 -Au nanoparticles.

Much like liver cancer, the mortality rate for colorectal (colon) cancer, among cancer-related deaths, is similarly high. The first-line chemotherapeutic drug for colorectal cancer treatment is 5-fluorouracil. Among 5-FU carriers, some contain the most abundant biopolymer—cellulose. It is characterized by good swelling properties, biocompatibility, and the ability of surface functionalization with different reactive groups, enabling effective drug loading. Recently, rice straw waste was used for cellulose isolation. Subsequently, magnetic cellulose bionanocomposites were fabricated for 5-FU loading and potential colorectal cancer treatment [80]. The 5-FU-loaded nanocarrier demonstrated better selectivity towards two colorectal cancer cell lines (HCT116, HT29) compared to colon normal cell lines than the pure drug. In vitro studies in tumor spheroidal models suggested effective penetration of the magnetic carrier into the tumors. Caspase assay indicated that the drug-loaded carrier could induce apoptosis in both colorectal cancer cells, while mitochondrial membrane potential assay showed a slight impact on mitochondrial function. The toxicity to red blood cells was insignificant. However, the anticancer activity in a model mimicking tumor–vasculature–drug interaction upon drug delivery was reduced (the percent inhibition below 50%) due to the tumor microenvironment, suggesting the need to improve the nanocarrier. Another 5-FU targeted delivery system comprised a magnetic triblock (PEG- poly- ϵ -caprolactone, PCL-PEG) copolymer with conjugated folic acid as a targeting ligand [81]. PCL hydrolyzes to 6-hydroxycaproic acid, a natural metabolite in the body, but the process is very slow. PCL copolymerization with PEG should ensure crystallinity, permeability, and polymer solubility, resulting in faster degradation. The

drug release was prolonged, which suggested a 5-FU location in the core region. The inhibitory effect of the 5-FU-loaded nanocarrier was investigated against different colon cancer cell lines (HCT116, SW480, HT29, Caco-2). The half-maximum inhibitory concentration values of the drug-loaded material for colon cancer cells were significantly lower than that of free 5-FU. Therefore, reduced drug doses could be used to inhibit cancer cells. The quantitative in vitro cellular uptake was evaluated by measuring Fe concentration, while in vivo studies were carried out by comparison of colon tumor tissues. The average iron content in HT29 cell lines, considered the most 5-FU-resistant colon cancer cell line, was about four times higher than in normal cells, reflected by the carrier accumulation in tumor tissue. Folate-mediated endocytosis was indicated as dominant in HT29 cells. This ligand–receptor interaction is considered a more efficient endocytosis type for drug distribution in colon tumors. Additionally, a significant inhibition of tumor volume was observed after 30 days, and the survival time of tumor-bearing mice was higher (48 days) than for mice treated with pristine 5-FU. Further research on this system was intended for targeted magnetochemotherapy [82].

There are also limited reports employing alternative active substances against colon cancer cells. Chitosan-coated magnetite nanoparticles were applied for targeted delivery of oxaliplatin (OXA) and irinotecan (IRI) [83]. However, the magnetite nanoparticle synthesis protocol assumed a coprecipitation method with chia seed mucilage as a capping agent in water. The preliminary studies using CT26 colorectal cancer cells showed promising anticancer activity of the OXA-IRI-loaded nanocarrier. Another polysaccharide, pectin (PET), was adopted for the preparation of oral magnetically driven PET nanoparticles for chlorogenic acid (CGA) targeted delivery to colon cancer (Figure 6) [84]. The magnetite covered with oleic acid ($\text{Fe}_3\text{O}_4@OA$) was responsible for magnetic response, while citrus pectin was responsible for CGA encapsulation. Pectin can effectively bind drugs through different bonds (covalent, ionic, hydrogen) and prevents drug release due to gelation and crosslinking. However, it is sensitive to pectinase produced in the colon. The proposed mechanism assumes that the orally administrated nanocarrier is targeted to the colon by external magnetic field. During PET/CGA/ $\text{Fe}_3\text{O}_4@OA$ movement, the outer layer of pectin protects CGA from an acidic environment of upper gastrointestinal track (stomach, small intestine), and finally the nanocarrier degrades in the colon due to pectinase, resulting in the drug release.

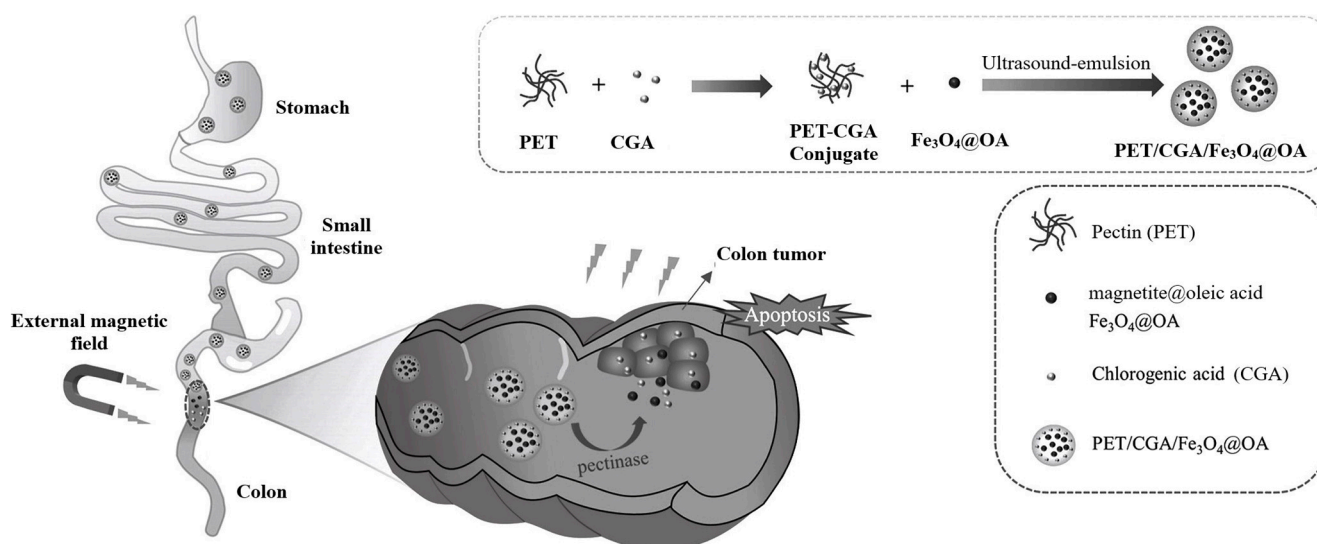


Figure 6. The synthetic procedure and proposed mechanism of chlorogenic acid's oral magnetically driven delivery system. Adapted from [84], Copyright (2023), with permission from Elsevier.

Cervical cancer is the fourth most common malignant gynecological tumor in women, and nearly 50% of cases affect women under 58 [85]. There have recently been few

reports of new magnetic carriers for targeted therapy in this area. For this purpose, magnetite was initially covered with a silica layer and then combined with a metal-organic framework—mesoporous zeolitic imidazole framework -8 (ZIF-8)—to increase drug loading capacity. Subsequently, chitosan functionalized with a targeted ligand (folic acid) covered a magnetic core, and cisplatin (CPT) was loaded into the nanocomposite [86]. ZIF-8 is often studied as a versatile nanocarrier characterized by biocompatibility and biodegradability in acidic environments. Chitosan should increase magnetic core stability and bioavailability, while FA improves targeting efficiency. A murine tumor model proved the inhibition effect of CPT-loaded nanocarrier on cervical tumor growth, and the anticancer activity was higher than that for pure cisplatin. Moreover, the drug enclosed within the delivery system primarily accumulated at the tumor site due to enhanced tissue necrosis in the cervical tumor compared to pristine CPT.

Folic acid was also attached as a targeting molecule to folate receptors to a magnetite core covered with hyperbranched glycerol (HPG) for curcumin delivery to cervical cancer [87]. Curcumin demonstrates the ability to damage HeLa cells, increasing reactive oxygen species generation and reducing the viability of cervical cancer cells. However, it requires protective carriers to increase its bioavailability and reduce high metabolism. HPG is a biocompatible polymer with a dendrimer-like structure that can be easily functionalized with targeting agents. The morphology of cells has not changed in the presence of the nanocarrier, but it has a negative impact on cell walls (normal and cancer cells) because cells aggregate due to electrostatic interactions. The CUR-loaded nanocarrier demonstrated considerable cell toxicity to tumor cells, which was time-dependent, and more toxicity was evaluated after 72 h than 24 h. The presence of FA increased selectivity towards cancer cells and cellular uptake. MRI studies showed the largest change in a reduction in signal enhancement in the HeLa cell line incubated with the CUR-loaded nanocarrier compared to other samples incubated with free CUR and the CUR-loaded nanocarrier without FA. It confirmed the observation from cellular uptake and cell viability studies.

Another proposed solution involving FA concerns the delivery of doxorubicin using magnetite connected by a disulfide bridge to chitosan functionalized with folic acid [88]. A disulfide bond is relatively stable in low concentrations of glutathione (GSH), characteristic of extracellular fluids (2 μM). However, it is destroyed via redox reaction in higher GSH concentrations (2–10 mM in intracellular fluids). Importantly, GSH concentration in cancer cell cytoplasm is at least four times higher than in normal cells. In turn, chitosan with easily protonated amine functional groups upon acidic conditions acts as a pH-responsive polymer that entraps the active agent in its porous channel in physiological pH and releases the drug in an acidic tumor environment. Folate receptors mainly mediated the nanocarrier internalization. The DOX-loaded dual-responsive system inhibited tumors significantly, and the cellular uptake by HeLa cells was much higher than that of normal cells. Although pure DOX demonstrated better inhibition properties, it also caused a high bodyweight mass decrease in mice, suggesting systemic toxicity.

In the case of bone cancer, the most common form in adults and children is osteosarcoma. The treatment of this cancer usually involves surgery and high doses of drugs, e.g., doxorubicin. Therefore, several nanocomposite systems were recently proposed for targeted delivery of active agents to the human osteosarcoma cell line (MG63). A magnetite-chitosan core-shell nanosystem was designed for DOX delivery to the MG63 cells by modifying chitosan with carboxylic acid functional groups participating in stable inclusion complex formation between Fe_3O_4 and chitosan [89]. Additionally, folic acid was conjugated to the nanocarrier for targeting folate receptors. The DOX-loaded material (high DOX concentration, 20 μM) was capable of osteosarcoma cell inhibition after 72 h (>60% cytotoxicity). The presence of FA resulted in a higher percentage of apoptotic cells in the DOX-loaded nanocarrier-treated MG 63 cells. According to a flow cytometric study, those cells could uptake more drug-loaded material than normal cells. After 4h of incubation, the cellular uptake was 85.46% for the material studied, while it was much lower for pristine DOX (38.19%) and slightly lower for the reference nanocarrier without folic acid (78.52%).

Another strategy for improving DOX delivery to bone-related cancer was based on magnetite encapsulated in bioactive glass (BG), additionally functionalized with reactive amine groups [90]. BG particles are biodegradable and biocompatible because they are capable of bonding to the bone via forming a hydroxycarbonate apatite layer. Importantly, the biodegradation products (Ca, P, Si) demonstrate osteogenic potential. The nanocarrier $\text{Fe}_3\text{O}_4@BG$ is proposed as a potential filler in bone cavities affected by bone tumors. It had no significant effect on cellular growth in lower concentrations, while above $250 \mu\text{g}/\text{mL}$, a significant reduction in cell proliferation was observed. It was attributed to the degradation of BG inside cells, resulting in an influence on cell homeostasis (presence of BG ionic degradation products). DOX release from the $\text{Fe}_3\text{O}_4@BG$ nanocarrier was pH-dependent. It was relatively slow in physiological conditions due to hydrogen bonds and electrostatic interaction between DOX and amine groups at the BG mesoporous surface. On the contrary, in an acidic environment, the protonated groups tended to be separated due to repulsive forces, resulting in faster drug release.

On the other hand, a magnetic nanocarrier composed of Fe_3O_4 and amine-functionalized β -cyclodextrin grafted graphene oxide was used for co-delivery of doxorubicin and melatonin (MLT) to increase apoptosis of osteosarcoma cells [91]. The composite nanocarrier was obtained in several synthetic steps. β -CD was functionalized with pH-responsive dendrimer with amine functional groups. Then, it was grafted with graphene oxide to obtain a platform with different functional groups. In the final step, magnetic NPs were synthesized on this platform. The cell viability did not fall below 85% at all treated doses of the nanocarrier (10 – $1280 \mu\text{g}/\text{mL}$). The co-delivery of DOX and MLT resulted in a synergistic antitumor effect because iMLT effectively protected normal cells against DOX cytotoxicity while enhancing antibiotic toxicity to cancer cells. The properties of β -CD were also applied for paclitaxel encapsulation in $\text{Fe}_3\text{O}_4@ \beta$ -CD nanopowders and thin films deposited by the matrix-assisted pulsed laser evaporation (MAPLE) technique [92]. The PTX-loaded films decreased the MG 63 cell viability by 85%.

There is considerably less focus on targeted magnetite-based systems for drug delivery in treating cancers other than those mentioned above, but there are several noteworthy solutions have been proposed. Albumin–perfluorohexane (PFH)–magnetite nanoparticles were produced for cisplatin delivery to gastric cancer cells [93]. PFH is widely used as an oxygen carrier to overcome hypoxic conditions and thus increase drug delivery to CPT-resistant cancer cells. The gastric cell growth inhibition strongly depended on the CPT dose on the magnetic nanocarrier, but the presence of protein coating increased the inhibition effect compared to free CPT. The enhanced induction of apoptosis resulted from the improved formation of intracellular reactive oxygen species. In turn, the system already mentioned several times, containing a cover composed of chitosan and polyethylene glycol, with conjugated folic acid, was also used to deliver PTX for fibrosarcoma—a rare cancer type affecting fibroblasts [94]. Again, the targeting ability of FA resulted in a higher uptake of PTX-loaded nanoformulation compared to free PTX and, subsequently, higher anticancer activity at the same dose. Additionally, tumor growth and volume were significantly reduced compared to free PTX. Folic acid was also included in aspartic acid-modified magnetite nanoparticles for DOX loading and potential application against skin cancer cell lines (B16-F1) [95]. The aspartic acid, a highly biocompatible molecule, contains two carboxylic acid groups facilitating DOX and Fe_3O_4 surface conjugation and an amine group for FA anchoring. Unlike the previously mentioned compounds for binding FA (natural/synthetic polymers), it is a relatively small particle without a negative impact on reducing the magnetization of magnetite nanoparticles. The DOX-loaded nanocarrier demonstrated cytotoxicity against the human skin cancer cell model. However, pure DOX was more toxic in lower concentrations due to the fast entry into the cell matrix. Among other anticancer drug delivery systems, pH-responsive chitosan-coated magnetic nanoparticles for telmisartan (TEL) delivery to prostate cancer cells [96] or silibinin (SIL) encapsulated in poly (lactic-*co*-glycolic) acid with magnetic core [97] for sustained drug delivery in renal cancer treatment can be mentioned.

Table 4. Recently described targeted drug delivery systems based on Fe₃O₄ NPs for potential application in treating different cancers.

Components of Magnetite-Based Delivery System	Cell Model	Characterization of Anticancer Properties	Loaded Drug/ Targeted Cancer	Reference
Dextran, polylactic acid	H22	Drug release, cytotoxicity In vivo: liver cancer inhibition	DOX/liver	[70]
Pluronic F127, polyethyleneimine	HepG2	Drug release, cellular uptake	DOX/liver	[71]
Boron nitride, polyethylene glycol	HepG2	Drug release, cytotoxicity, cellular uptake In vivo: tumor volume, histopathological studies	DOX/liver	[72]
Formyl deoxycholic acid, FA	HepG2	Drug release, blood compatibility, cellular uptake, cytotoxicity, apoptosis staining, Western blotting	DOX/liver	[73]
Zn-Al layered double hydroxide	HepG2	Drug release, cytotoxicity	DOX/liver	[74]
polyethylene glycol	HepG2	Drug release, cytotoxicity	SFB/liver	[75]
Polyethylene glycol	HepG2	Drug release, cytotoxicity, cellular uptake In vivo: under-skin implantation, 2D mapping, content in liver tissue	SFB/liver	[76]
Polyvinyl alcohol, Zn-Al layered double hydroxide	HepG2	Drug release, cytotoxicity	5-FU/liver	[77]
Polyethylene glycol, crocetin	HepG2	Drug release, cytotoxicity	CRT/liver	[78]
Polyethylene glycol, Au, monoclonal antibodies	-	Drug release In vivo: histopathological studies	AVS/liver	[79]
Cellulose	HCT116 HT29	Drug release, cytotoxicity, cell vitality, apoptosis induction, mitochondrial function, magnetic targeting	5-FU/colon	[80]
Polyethylene glycol, poly-ε-caprolactone, FA	HT29 Caco-2 SW480 HCT116	Drug release, cytotoxicity In vivo: cellular uptake, tumor volume, Western blotting	5-FU/colon	[81]
Chitosan	CT26	Cell viability	OXA&IRI/colon	[83]
Oleic acid, pectin	HCT116	Drug release, cytotoxicity, cellular uptake	CGA/colon	[84]
Silica, ZIF-8, chitosan, FA	TC1	Drug release In vivo: antitumor activity, pronecrotic effect	CPT/cervical	[86]
Polyglycerol, FA	HeLa	Drug release, cytotoxicity, cellular uptake	CUR/cervical	[87]
Oleic acid, chitosan, FA	HeLa	Drug release, cytotoxicity, cellular uptake In vivo: antitumor activity	DOX/cervical	[88]
Chitosan, FA	MG63	Drug release, cell viability, cellular uptake, apoptosis induction	DOX/ osteosarcoma	[89]
Bioactive glass	MG63	Drug release, cell viability, cellular uptake	DOX/ osteosarcoma	[90]
Graphene oxide, β-cyclodextrin	Saos2 MG63	Drug release, cytotoxicity, cellular uptake, apoptosis induction, expression levels	DOX&MLT/ osteosarcoma	[91]
β-cyclodextrin	MG63	Cell viability	PTX/ osteosarcoma	[92]
Albumin, perfluorohexane	AGS	Drug release, cytotoxicity, apoptosis induction	CPT/gastric	[93]
Chitosan, polyethylene glycol, FA	WEHI164	Drug release, cytotoxicity, apoptosis induction In vivo: tumor volume	PTX/ fibrosarcoma	[94]
Aspartic acid, FA	B16 F1	Drug release, cytotoxicity	DOX/skin	[95]
Chitosan	PC 3	Drug release, cytotoxicity	TEL/prostate	[96]
Poly (lactic-co-glycolic) acid	A 498	Drug release, cytotoxicity In vivo: acute toxicity	SIL/renal	[97]

4. Multifunctional Magnetite-Based Nanomaterials

Although chemotherapy is the most often used conventional method in cancer treatment, its capability to kill tumor cells is often insufficient. Therefore, many multifunctional solutions are proposed to increase anticancer efficiency. Magnetite nanoparticles (MNPs) in the targeted delivery systems allow for chemotherapy to be combined with other methods. Some of the previously cited original papers also explored additional properties of magnetite-based nanosystems. Nevertheless, the primary emphasis was on its potential application in chemotherapy. Hence, the subsequent discussion on nanomaterials will revolve around multifunctional systems integrating chemotherapy with magnetic hyperthermia (MHT), photothermal therapy (PTT), or magnetic resonance imaging (MRI) (Table 5).

In some reports, the application of hyperthermia is reduced to simple heating of samples. This procedure was used to investigate the properties of a magnetic hydrogel based on tragacanth gum [98]. The magnetite nanoparticles functionalized with amine group and folic acid were incorporated into tragacanth gum-g-polyacrylic acid copolymer crosslinked with cystamine to create a pH- and redox-responsive platform for DOX delivery. The combination of chemo and hyperthermia therapy consisted of cytotoxicity studies carried out for temperature raised to 45 °C in the last 2 h. The MCF 7 breast cancer cells were used for cell viability studies, and the results after 24 h showed better efficiency of pure DOX due to its burst accessibility. However, after 48 h, the DOX-loaded nanocarrier demonstrated higher anticancer performance, which was slightly improved by increasing temperature. Similarly, the same research group investigated the MCF 7 cell viability at 37 and 45 °C in the presence of another DOX-loaded magnetic hydrogel containing host molecule β -cyclodextrin (β -CD) and poly(2-ethyl-2-oxazoline) (PEtOx), ionized at the acidic cancerous environment and facilitating drug release [99]. Again, a similar anticancer activity trend was observed for free DOX, DOX-loaded hydrogel, and combining chemotherapy with hyperthermia after 24 and 48 h. On the other hand, the anticancer activity of the DOX-loaded alginate-based hydrogel was investigated in the presence of an alternating magnetic field (AMF) [100]. The potential intratumoral hydrogel included poly(lactic-co-glycolic acid) (PLGA) for DOX loading and Fe₃O₄ NPs as heating agents entrapped in the alginate matrix. The nanocarrier could generate heat when subjected to AMF, and the temperature increase depends on the concentration of magnetite nanoparticles in the hydrogel. After 10 min of AMF application, the hydrogel temperature increased by 4.82 and 16 °C at the magnetite concentrations of 1 mg/mL and 4 mg/mL, respectively. The A549 lung cancer cells demonstrated significantly lower viability after 24 h incubation with the DOX-loaded hydrogel followed by 30 min of AFM exposure (42.92%) compared to the samples without AMF exposure (61.57%). The *in vivo* studies also confirmed the beneficial effect of heat generation by magnetite NPs on the tumor side. The tumor size ($[\text{width}^2 \times \text{length}]/2$) after treatment for 28 days was 1.76 and 0.46 for using only chemotherapy and combined chemotherapy with AMF, respectively, while the reference tumor (no treatment) demonstrated an average size of 3.28.

Combining active drug targeting with near-infrared region (NIR, 750–1200 nm) responsiveness is another strategy for improving anticancer therapy. For this purpose, magnetite-modified graphene oxide was coated with folic acid-grafted maltodextrin [101]. The photothermal effect was studied using different concentrations of the nanocarrier and NIR (808 nm) laser with different power intensities. It was found that the temperature changed from 21.6 to 61.5 °C as the nanosystem concentration was 0 and 1 mg/mL, respectively. A similar effect was observed for the increased laser power intensity, so the temperature for power 0.5 W/cm² increased to 41.5 °C and for power 2.0 W/cm² to 61.5 °C. Interestingly, the photothermal effect of magnetite or graphene oxide was similar and much lower than that of magnetic graphene oxide. The cytotoxicity studies without and with NIR stimulation confirmed the excellent conversion efficiency of the nanocarrier. The liver cancer cell viability in the presence of the nanocarrier combined with PTT was only 53.3%, while without PTT, the cell survival rate was very high (at least 80%). The DOX-loaded nanocarrier contributed to much lower cell survival (32.5%), which was addi-

tionally reduced by photothermal therapy (21.2%), confirming the advantage of combined therapies over single chemotherapy. Another nanoplatfrom dedicated to DOX delivery and liver cancer treatment comprised a magnetite core covered with a porous carbon(C)/ZnO structure with conjugated FA [102]. The photothermal effect was initially investigated in water for Fe₃O₄@C/ZnO-FA and C/ZnO nanocarrier using laser irradiation (638 nm, 1.0 W/cm²) and temperature increased by 17 and 15.6 °C, respectively. The *in vitro* studies of cell viability and *in vivo* tumor size proved the synergistic effect of DOX and PTT against liver cancer cells. The killing effect of DOX-loaded Fe₃O₄@C/ZnO-FA was very high (73%) but significantly improved (90%) under a 638 nm laser irradiation. Additionally, the mice treated with DOX-loaded Fe₃O₄@C/ZnO-FA + PTT had the longest survival time (12 days) and the highest survival rate (78%).

Another approach for synergistic liver cancer therapy was designed using crosslinked hydroxypropyl cellulose and carboxymethyl chitosan as an injectable hydrogel with loaded magnetite, photosensitizer black phosphorous (BP) nanosheets, and reactive agent artesunate (ART) [103]. ART is a first-line antimalarial drug, but it demonstrates auspicious anticancer properties as it inhibits the growth of hepatocellular carcinoma cells. The synergistic effect on tumors was studied using free ART, ART-loaded hydrogel, ART-loaded hydrogel+NIR, ART-loaded hydrogel+magnetic field (MF), and ART-loaded hydrogel+NIR+MF. In turn, camptothecin (CPT) was loaded into magnetic graphene oxide coated with a β -cyclodextrin–cholic acid (CA)–hyaluronic acid (HA) polymer for hepatocellular carcinoma therapy [104]. The material showed excellent photothermal stability and conversion efficiency as the solution temperature rose from 47 to 71 °C (from 0.1 to 1.0 mg/mL) upon NIR irradiation (808 nm, 15 min, 2.0 W/cm²). *In vivo* studies with tumor-bearing mice were carried out using different irradiation times (1–5 min), and the temperature of the tumor site grew to 58 °C. After 21 days of treatment, the group treated with CPT-loaded nanoplatfrom + NIR demonstrated the most substantial antitumor effect (90%).

Among the nanosystems dedicated to breast cancer therapy, magnetite-modified graphene oxide was again applied by Işıklan et al. [105]. After functionalization with hydroxypropyl cellulose and loading with PTX, it was tested in combined chemotherapy and PTT. The photothermal performance (808 nm, 1.0 W/cm², time 6–10 min) was investigated using different concentrations of the nanoplatfrom (Figure 7). The higher the concentration of the nanocarrier, the more significant the temperature increase. Finally, the temperature of the nanobiocomposite solution (1 mg/mL) increased from 18.2 to 59.8 °C after 10 min of laser irradiation, confirming excellent light-transform capability. On the other hand, liposomes containing magnetite and a cardiotoxic steroid—bufalin (BFL)—were investigated using different Fe₃O₄ concentrations (10–300 μ g/mL) [106]. The highest temperature of 72.3 °C was recorded for the highest concentration of the photothermal agent—magnetite NPs (5 min of irradiation, 808 nm, 2.0 W/cm²). Cytotoxicity studies confirmed the significant impact of NIR irradiation on 4T1 cell growth inhibition. It suggested that local heating facilitated BFL penetration and accumulation in cancerous cells. In turn, gelatin nanoparticles functionalized with folic acid were loaded with curcumin, magnetite NPs, and copper sulfide (CuS) [107]. CuS was responsible for an enhanced anticancer effect through NIR irradiation. Another solution involved generating local heat (MHT) in response to an alternating magnetic field (AMF) and laser (PTT) [108]. The nanoplatfrom for DOX delivery contained pH-sensitive poly(ethylene)glycol-poly(β -amino esters) and thermosensitive dipalmitoyl phosphatidylcholine. The inhibitory rate of cancer cells incubated with a DOX-loaded nanocarrier was 59.81%, which increased to 80.03% after combining MHT and PTT.

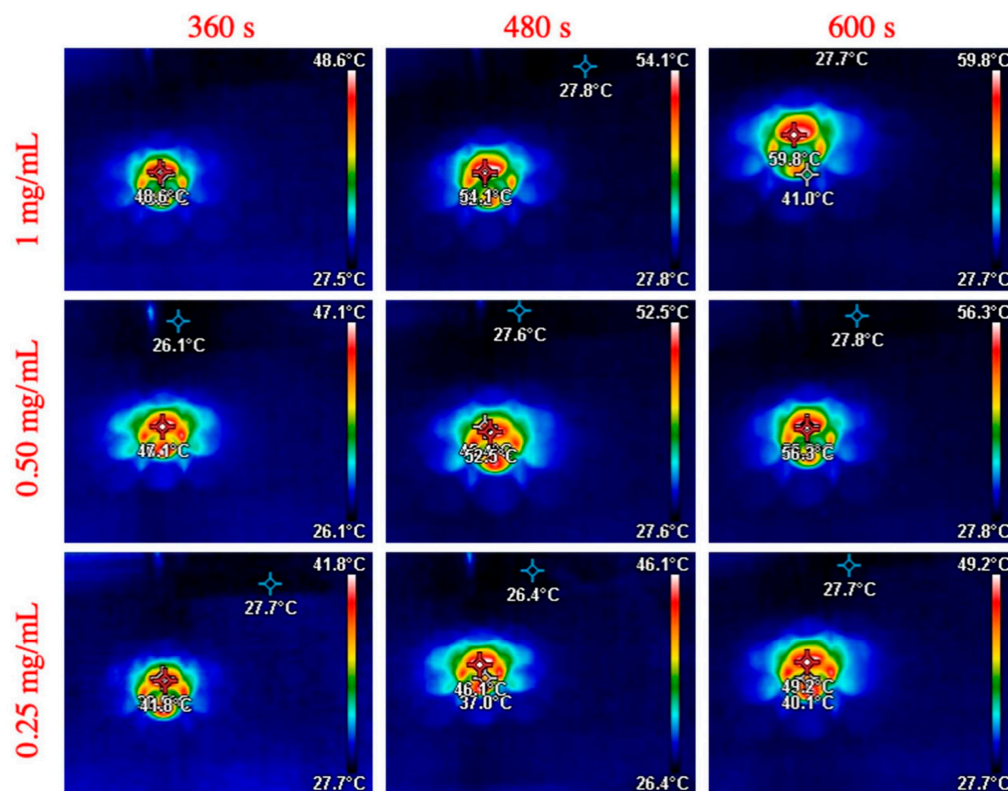


Figure 7. NIR thermographic images of PTX-loaded magnetite graphene oxide functionalized by hydroxypropyl cellulose (solutions 0.25–1 mg/mL) under NIR laser irradiation (808 nm, 1.0 W/cm²). Reprinted from [105], Copyright (2023), with permission from Elsevier.

Another group of multifunctional nanocarriers is designed to integrate chemotherapy and magnetic resonance imaging. A magnetic nanogel, loaded with DOX, was developed as a potential nanocarrier in HER2-positive breast cancer therapy and diagnostics [109]. The magnetic nanogel was composed of a magnetite and hydrogel hybrid structure with thermosensitive N-isopropyl acrylamide–acrylic acid, acrylic acid, and (ethylene glycol) methacrylate as hydrophilic monomers. Herceptin antibody, targeting human epidermal growth receptor factor 2 (HER2), was also conjugated. Magnetic nanogels have the potential to be applied as probes for MRI; thus, they were used as MRI contrast agents for tumor detection. In vivo T₂-weighted MR images of nude mice with breast tumors enabled the assessment of enhancement efficiency. A noticeable signal enhancement in the MCF-7 tumor region was observed after the nanogel administration, with a decrease in brightness due to magnetite NP accumulation and entering the tumor region. DOX-loaded nanogel showed a significant signal decrease as an effect of enhanced accumulation. The injection of DOX-loaded nanogel with conjugated Herceptin resulted in a higher brightness decrease, while the increase in the T₂ signal confirmed further tumor targeting and accumulation.

Other proposed nanocomposites for MRI, targeted DOX delivery, and cell labeling included an Fe₃O₄ core with attached carbon quantum dots [110]. The in vitro T₂-weighted MR images of water dispersed with the nanocarrier were taken for different Fe concentrations (0–0.6 mM). The MR signal intensity of T₂ images changed significantly with increasing iron concentration. Thus, the nanocarrier generated MR contrast due to dipolar interactions of the nanoparticle magnetic moment and protons in water. An analogous concentration-dependent darkening effect and high T₂-weighted MR images at low Fe concentration were observed for the nanosystem based on a magnetite core and double-layered organic shell (poly(glycidyl methacrylate–polyethylene glycol) and saiep dialdehyde) [111]. T₂ relaxation rates showed linearity with increasing Fe concentration (0.04–0.20 mM) and high transverse relaxivity (119 mM⁻¹s⁻¹). Another approach assumed magnetite core func-

tionalization with β -CD and further conjugation of cyclic 13mer oligopeptide Pep42 as a targeting agent to glucose-regulated protein 78 (GRP78) overexpressed in cancer cells [112]. The presence of loaded DOX and Pep42 resulted in a decrease in breast cancer cell viability and significant induction of apoptosis. The *in vitro* MRI studies, similar to the previous examples, showed that the nanocarrier could be suitable as a negative contrast agent. The *in vivo* MRI studies showed differences in the images before and after injection of the contrast agent (the nanocarrier). The values of negative contrast enhancement (NCE) were different for different times after injection, and the highest NCE level was observed after 1 h. A more detailed *in vivo* MRI analysis was performed on the composite system containing Fe_3O_4 /poly (ϵ -caprolactone) NPs functionalized with chitosan, (Fe_3O_4 /PCL)/CS for gemcitabine (GEM) delivery [113]. After the NP injection (Fe concentration of 5 mg/kg), rapid liver uptake occurred, manifested by a fast relative enhancement increase (40%) within 5 min. Lower uptake (about 20%) was observed for spleen and kidneys (Figure 8a–c). The analysis of T_2 -weighted images (Figure 8d–f) showed darker areas in the liver, kidneys, and spleen at 1 and 24 h post-injection. However, based on the quantitative analysis of the NPs biodistribution (T_2 -mapping), the liver and kidneys demonstrated a statistically significant increase in relaxivity R_2 ($1/T_2$), and the values of ΔR_2 were 3.9 and 8.0 s^{-1} after 1 h, while being 8.9 and 15.7 s^{-1} after 24 h, respectively (Figure 8g). Additionally, the changes observed in muscles were negligible.

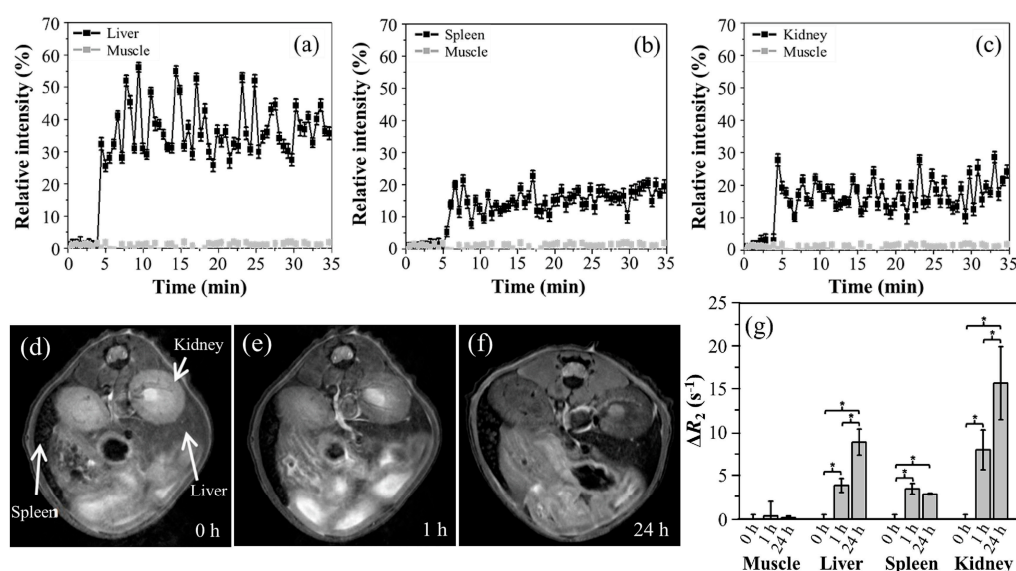


Figure 8. *In vivo* time courses of the (Fe_3O_4 /PCL)/CS NPs: (a) liver; (b) spleen; and (c) kidney. T_2 -weighted MR images of the kidney, spleen, and liver after the NPs injection at: (d) 0, (e) 1, and (f) 24 h. (g) ΔR_2 (s^{-1}) as a function of time of muscle, liver, spleen, and kidney after NP injection. The statistical test was significant for data with * ($p < 0.05$). Reprinted from [113], Copyright (2023), with permission from Elsevier.

Finally, it is essential to highlight multifunctional systems that integrate potential applications in chemotherapy, enhanced by heat generation (MHT, PTT), and diagnosis (MRI). Magnetic nanorings— Fe_3O_4 @polyvinylpyrrolidone (PVP)—loaded with doxorubicin were applied for synergetic magnetic hyperthermia and chemotherapy [114]. The investigation of MHT was additionally carried out using two types of magnetite nanoparticles—*isotropic* superparamagnetic (SNPs) and *anisotropic* ellipsoid ferrimagnetic (FNPs)—as reference samples. Under the same AMF, the temperature rises to 12.5, 27, and 33 $^{\circ}\text{C}$ for SNPs, FNPs, and the nanorings, respectively. The *in vivo* MHT studies were investigated after direct injection of the DOX-loaded nanocarrier. The local temperature was raised to 44 $^{\circ}\text{C}$ under AMF. On the other hand, the *in vitro* T_2 MR images tended to darken with increasing Fe concentrations; thus, the nanocarrier could expand the ^1H spin relaxation time (negative

contrast agent). The in vivo animal experiments proved the synergistic effect of heat therapy and DOX release in inhibiting tumor growth without side effects. Another approach was based on magnetite NPs stabilized by different plant extract concentrations (*Punica granatum* fruit peel) [115]. The maximum temperature rise under AMF was observed for the lowest extract concentration, and it increased with increasing AMF strength (up to 54 °C). However, only the highest extract concentration (8%) guaranteed the secure hyperthermia range. According to the in vitro MRI studies, the relaxivity increased with increasing concentration, while the extract showed almost no value. Another interesting multifunctional nanopatform, Au NPs loaded on mesoporous magnetite nanospheres, combined chemotherapeutic activity improved by NIR laser irradiation with MRI diagnostics [116]. A more advanced nanosystem for simultaneously therapeutic and diagnostic properties was designed for multimodality imaging and synergistic chemo–photothermal therapy [117]. PEGylated poly(lactic-co-glycolic acid) microcapsules were used to load DOX and Prussian blue photothermal agent. The core–shell structure demonstrated excellent photothermal conversion properties, which resulted in much higher tumor inhibition efficiency, but also was capable of simultaneous enhancement in ultrasound imaging (USI), photoacoustic tomography (PAT), and MR imaging.

Table 5. Multifunctional magnetite-based nanosystems for potential application in the treatment of different cancers.

Components of Magnetite-Based Delivery System	Application in Cancer Therapy *	Loaded Drug/Targeted Cancer	Reference
Tragacanth gum, poly acrylic acid, cystamine, FA	HT	DOX/breast	[98]
β-cyclodextrin, poly(2-ethyl-2-oxazoline)	HT	DOX/breast	[99]
Poly (lactic-co-glycolic acid), alginate	MHT	DOX/lung	[100]
Graphene oxide, maltodextrin, FA	PTT	DOX/liver	[101]
Carbon, ZnO, FA	PTT	DOX/liver	[102]
Hydroxypropyl cellulose, carboxymethyl chitosan, black phosphorus	PTT	ART/liver	[103]
Graphene oxide, β-cyclodextrin, cholic acid, hyaluronic acid	PTT	CPT/liver	[104]
Graphene oxide, hydroxypropyl cellulose	PTT	PTX/breast	[105]
liposome	PTT	BFL/breast	[106]
Gelatin, CuS, FA	PTT	CUR/breast	[107]
Poly(ethylene)glycol-poly(β-amino esters), dipalmitoyl phosphatidylcholine	MHT, PTT	DOX/breast	[108]
Poly(<i>N</i> -isopropylacrylamide-acrylic acid-(ethylene glycol) methacrylate), herceptin	MRI	DOX/breast	[109]
Carbon quantum dots	MRI	DOX/breast	[110]
Poly(glycidyl methacrylate-polyethylene glycol), salep dialdehyde	MRI	DOX/breast	[111]
β-cyclodextrin, Pep42	MRI	DOX/breast	[112]
Poly (ε-caprolactone), chitosan	MRI	GEM/breast	[113]
Polyvinylpyrrolidone	MRI, MHT	DOX/osteosarcoma	[114]
<i>Punica granatum</i> fruit peel extract	MRI, MHT	5-FU/colorectal	[115]
Gold nanoparticles	MRI, PTT	DOX/cervical	[116]
Polyethylene glycol, poly(lactic-co-glycolic acid), Prussian blue	MRI, PAT, USI, PTT	DOX/osteosarcoma	[117]

* Each drug delivery system demonstrates potential application in chemotherapy.

5. Monitoring of Magnetite-Based Nanocarriers Interacting with Cells in Biological Systems

Transferring research on magnetite-based nanosystems from the academic laboratory level to practical biomedical applications requires an actual analysis of the processes that nanocarriers undergo in biological systems. In general, the mechanisms proposed for the delivery of magnetic nanostructures assume using a strong magnetic field near the target site after DDS injection or implantation of magnets near the target tissue before injection. In practice, the first method encounters difficulty in penetrating deep tissues by an external magnetic field, and the second method requires knowledge of the exact location of cancer cells. Moreover, only a few original works thoroughly examine this issue [38,55,76]. Typically, articles describe the magnetic properties of a drug nanocarrier using a magnetometer, and the efficacy of targeted drug delivery therapy is assessed solely based on the magnetic saturation values. Then, it is often assumed that an external magnetic field generated by permanent magnets, along with a gradient, would be capable of concentrating the drug at the tumor site or other target tissues. However, the magnetic field is able to penetrate the body up to 2 cm from the skin, and its strength is reduced with distance; thus, efforts are underway to explore minimally invasive solutions [118–120]. Recently, a new method for focusing magnetic nanoparticles in three-dimensional space was proposed [121]. The focusing system was based on four neodymium magnets in a special configuration rotating around a sample with magnetic particles. Two magnets (magnetic induction 60 mT; diameter 70 mm) produced a strong homogeneous magnetic field of N-S, while two others (magnetic induction 30 mT; diameter 35 mm) produced a magnetic field of opposite orientation. The magnet system rotating around a sample containing ferromagnetic particles led to a rapid concentration of those particles in a three-dimensional space. Hence, this approach can potentially concentrate a magnetic drug carrier in a specific area, facilitating the release of an optimal drug dosage. The method was also applied to investigate the effect of different organic units attached to the magnetite core on the average focusing time in a saline–serum mixture [122]. The highest focusing time was observed for magnetic NPs with amine, carboxylic groups, and quaternary ammonium salts. It is presumably the effect of the strongest interactions of those groups with bioorganic molecules present in serum compared to other organic units. These findings could be significant in determining the focusing mechanism of nanoparticles as the functional groups at the surface of the magnetite core significantly influence the rate of their concentration in a desired area.

On the other hand, extensive *in vitro* research is being carried out on monitoring cells interacting with magnetic nanocarriers in biological systems. However, it is also crucial to investigate nanoparticles upon their introduction into a biological system [25,123,124].

Initially, biomolecules interact with a magnetic NP's surface through physical adsorption (ionic, electrostatic interactions, van der Waals forces) or chemical linkages (covalent bond). However, within the discussed nanosystems, many have been specifically engineered to exhibit a higher binding affinity towards cells. The presence of targeted ligands (e.g., FA) at the nanocarrier surface results in ligand–receptor interactions characterized by higher bond strength. Another strategy is an attachment on the NP's surface special functional groups (e.g., thiol), which results in chemical conjugation with cells.

The adsorption at the NPs involves different functional groups, depending on the biomolecule: carboxylic groups in proteins; hydroxyl, amino, and carboxylic in carbohydrates; phosphate in DNA; carboxylic and phosphate in lipids. Although various biomolecules interact with the surface of NPs, proteins surround the surface immediately after NPs are introduced into the biological system, forming protein corona. The interactions on the protein–NP surface are dynamic, with continuous adsorption/desorption processes. The presence of proteins results in the surface modification of NPs and, consequently, their bioreactivity. Thus, this is an essential aspect determining the recognition of magnetic nanocarriers by cells and their further cellular internalization. Meanwhile, research is most often carried out confirming only the formation of protein corona (e.g., with

human serum albumin) without further examination of this issue. In drug delivery systems, effective treatment relies significantly on the cellular uptake of drug-loaded nanocarriers. They primarily gain entry into the cells through endocytosis, as confirmed by transmission electron microscopy (TEM) [125]. The potential entry mechanisms vary based on the size of nanoparticles. Endocytosis can be categorized into two primary types: phagocytosis, typically associated with the uptake of particles larger than 0.5 μm in diameter, and pinocytosis, encompassing macropinocytosis, clathrin-mediated endocytosis, caveolin-mediated endocytosis, and clathrin/caveolae-independent endocytosis. Particles exceeding a diameter of 200 nm are commonly internalized through the processes of phagocytosis or micropinocytosis mentioned above. Nanoparticles with a diameter below 10 nm and cationic nanoparticles, characterized by high charge density, gain entry into the cell through direct penetration and pore formation. Numerous approaches have been suggested and employed to investigate endocytosis processes. These methods encompass chemical and pharmacological inhibitors, specific biomarkers, genetic techniques, and diverse microscopy techniques such as fluorescence, electron, and atomic force microscopy [126–128].

The characteristics affecting the penetration of nanoparticles into cells or tissues are associated with their size, surface charge, and hydrophobicity [129]. Therefore, nanoparticles exceeding 150 nm in diameter typically accumulate in the spleen and liver; those within the 30–150 nm range in the bone marrow, stomach, heart, and kidneys; and those smaller than 20 nm primarily gather in the kidneys. Additionally, research indicates that positively charged and hydrophobic particles have shorter circulation times than their hydrophilic and negatively charged counterparts [130]. Other crucial factors include biocompatibility, bioaccumulation, colloidal stability, solubility, administration method, degradation rate, and the target cell/tissue [127]. The factor that can halt endocytosis is an initial incubation temperature of 4 °C. Subsequently, unbound nanoparticles are removed through washing, and the incubation temperature is reverted to 37 °C. It facilitates a more straightforward interpretation of internalization kinetics [126].

On the other hand, nanoparticles face challenges within the human body due to physiological barriers. Initially, when nanoparticles are injected into the bloodstream, they can accumulate, altering their magnetic properties and impeding further movement. The already mentioned protein corona can potentially lead to their aggregation before reaching the cell [126]. Additionally, their interaction with plasma proteins may trigger immune responses. Further limitations arise from the relationship between particle size and the anatomy of the target tissue. Within the brain, the rate of pinocytosis is restricted, and the robust intercellular connections forming the blood–brain barrier (BBB) hinder the passage of small particles possessing suitable physicochemical properties [129]. Additional constraints arise from intracellular barriers, encompassing challenges such as lysosome and endosome degradation escape, as well as physiological factors like target tissue characteristics, blood flow in the area, vascular sources, body weight, method of nanoparticle injection, distance from the field source, and tumor volume. The accumulation of nanoparticles is also linked to a higher enhanced permeability and retention (EPR) rate in cancer cells and tissues, occurring more rapidly than in healthy counterparts. Studies have demonstrated that nanoparticles ranging in size from 10 to 100 nm tend to accumulate predominantly in tumors as opposed to healthy cells and tissues [130].

In the context of utilizing magnetic nanoparticles for diagnostics and therapy, the optimal approach for their studying in biological systems is to integrate imaging techniques that facilitate their visualization with those employed for the pathological examination of tissues. Various imaging techniques, such as magnetic resonance imaging (MRI) and positron emission tomography (PET), have been extensively utilized to track the targeting and biodistribution of nanoparticles throughout the entire body [13,112,113]. On the other hand, magnetic particle imaging (MPI) enables the direct detection of the quantity and location of superparamagnetic nanoparticles within biological tissue, surpassing the sensitivity of MRI [129].

Other methods are employed for smaller areas. Fluorescence microscopy, both conventional and confocal, is one of such methods, chosen for its relatively straightforward experimental setup. Its utilization was identified in numerous original papers referenced in this review [46–48,50,51,63,71,73,80,84,88,90,95,101–104,110,117]. It allows for studying extensive cell populations or relatively sizable tissue samples. However, its resolution (approximately 200 nm) does not allow for the observation of individual nanoparticles and their interactions with cells and specific tissue components. Moreover, the observed structures must undergo fluorescent labeling, introducing the risk of altering their bioreactivity. Another difficulty lies in the precise differentiation between nanoparticles bound to the plasma membrane and those internalized [125]. A similar issue pertains to flow cytometry (FC), a method used to quantify the association of nanoparticles with cells [89,91,103,107–109]. However, it quantifies the total association and does not distinguish between internalized material and surface-bound particles. Flow cytometry holds the advantage of simultaneously observing numerous cells and fluorophores. Additionally, there have been recent advancements with improved resolution, including total internal reflection fluorescence microscopy (TIRF), illumination microscopy (SIM), expansion microscopy (ExM), and single-molecule localization microscopy (SMLM) [126].

Another method within electron microscopy is scanning electron microscopy (SEM). While it boasts high resolution (3–20 nm), it is limited to imaging only the sample's surface. In this context, SEM primarily characterizes the spatial relationship between nanoparticles and the cell surface. In turn, confocal laser scanning microscopy (CLSM) offers a spatial representation of cells and their constituents growing *in vitro* on 3D scaffolds [55,65,117]. On the other hand, transmission electron microscopy (TEM) is a robust technique for obtaining information on nanoparticle uptake, biodistribution, and interactions with cell and tissue components. While the achievable resolution is approximately 0.2 nm, the practical limitations imposed by preparing biological samples restrict the resolution to around 2 nm. Furthermore, observations can only be carried out on thin and small sample slices. An additional drawback is the limitation of obtaining only static information. Conversely, the benefits encompass the capability to detect nanoparticles in cells and tissues and the acquisition of qualitative and quantitative data on their chemical composition. TEM can be integrated with other techniques to enhance its utility. Correlative light and electron microscopy (CLEM) aligns the overall cellular view with detailed information from TEM. Addressing the issue of thin samples, scanning transmission electron microscopy (STEM) offers a spatial resolution of 5–10 nm [127].

Various microscopic techniques have been employed to quantify iron oxide nanoparticles and assess their 3D distribution within cells and tissues. In investigations involving cells and superparamagnetic iron oxide nanoparticles, TEM and 3D electron tomography can be utilized. Another approach to gaining insights into the 3D interaction between iron oxide NPs and cancer cells involves combining TEM with cryo-soft X-ray tomography. Additionally, the 3D distribution of magnetite nanoparticles, coated with a fluorescent unit, within the intracellular environment could be determined using fluorescence microscopy in conjunction with scanning transmission X-ray tomography and ptychography. A study of iron oxide nanoparticles with cells employed a combination of scanning transmission electron microscopy (STEM), electron tomography, and EDX chemical analysis. Moreover, effective detection of magnetic nanoparticles in cancer cells can be achieved using electron spectroscopic imaging (EELS) combined with STEM [125].

Among other methods, atomic force microscopy (AFM) is worth mentioning for the visualization of single molecules and cells. The samples in liquid environments can be observed with sub-nanometer resolution. To enhance its capabilities, AFM can be synergistically integrated with fluorescence microscopy and total internal reflection fluorescence (TIRF). It facilitates a more comprehensive characterization of single-molecule structures and dynamic interactions [127]. Moreover, magnetic relaxometry (MRX) is another method capable of detecting and locating magnetic nanoparticles. For medical usage, it is crucial to specify the size of the nanoparticles (typically in the order of tens of nanometers) and ensure

they possess high magnetic moments [129]. Finally, Raman microscopy can also be used to observe nanoparticles inside cells and give information on biochemical interactions within the cells. Surface-enhanced Raman scattering (SERS) is a non-destructive and water-free interference technique appropriate for biological samples [131].

Endocytosis can also be examined at the levels of protein and gene expression. Inhibitors that block endocytosis are employed. However, this approach may introduce potential side effects, such as cytotoxicity and the upregulation of the entire process. Genetic approaches offer greater specificity than chemical inhibitors, yet they have certain limitations. Hence, it is advisable to combine various approaches and controls. The examination of protein levels (proteomics) is carried out using mass spectrometry (MS). Studies at this level yield extensive information about endocytosis processes and other cellular biological processes linked to cell proliferation, inflammation, and apoptosis [127].

The structure and dynamics of proteins and nucleic acids for endocytosis can be studied by electron spin resonance (ESR) spectroscopy and confocal laser scanning microscopy [132]. Nevertheless, investigations utilizing ESR and associated techniques involve using stable free radicals known as spin labels—stable free radicals that can also serve in functionalizing magnetic nanoparticles [133,134].

The discussion on the interactions between nanoparticles and cells is closely related to reactive oxygen species (ROS), which are intracellular free radicals characterized by one or more unpaired electrons in their valence shell [135]. ROS can originate from both exogenous and endogenous sources, with mitochondria as one of the primary endogenous contributors within a cell [136]. The direct technique for investigating free radicals, including ROS, is electron spin resonance. As the production of ROS predominantly takes place in mitochondria, employing this method provides a valuable opportunity to monitor interactions between different molecules, including nanoparticles and cells. The ESR method investigated the interaction between magnetic nanoparticles functionalized with spin labels with yeast and cancer cells. 2,2,6,6-Tetramethylpiperidine 1-oxyl (TEMPO) and 4-Hydroxy-2,2,6,6-tetramethylpiperidine-1-oxyl (4-Hydroxy-TEMPO, TEMPOL) spin probes can interact with free radicals and are considered potential scavengers for these radicals [133–135]. Based on alterations in the shape and intensity of the ESR signal, it is possible to differentiate such molecules (whether free or attached to magnetite nanoparticles) located outside a cell, within the cell membrane, and inside a cell. Figure 9 shows changes in the structure and intensity of ESR spectra of a TEMPOL spin label attached to magnetite-based NPs loaded with doxorubicin ($\text{Fe}_3\text{O}_4@\text{SiO}_2@\text{SiNHDOX}@\text{Dextran-TEMPOL}$) [134]. The nanoparticles incubated with cells were monitored over time by analyzing changes in ESR spectra. The ESR signals from TEMPOL spin labels vary based on the nanoparticles' location within the cell. The primary advantage of this method, in contrast to those mentioned earlier, lies in its capability to observe and monitor both the dynamic and static aspects of the endocytosis process, including the entry of nanoparticles into the cells. An additional benefit of this method is that the samples do not necessitate any specific preparation. Spin labels can be broadly applied to various types of nanomaterials, and the study of endocytosis using the ESR technique is ongoing, including its application in a free form without nanomaterials [137].

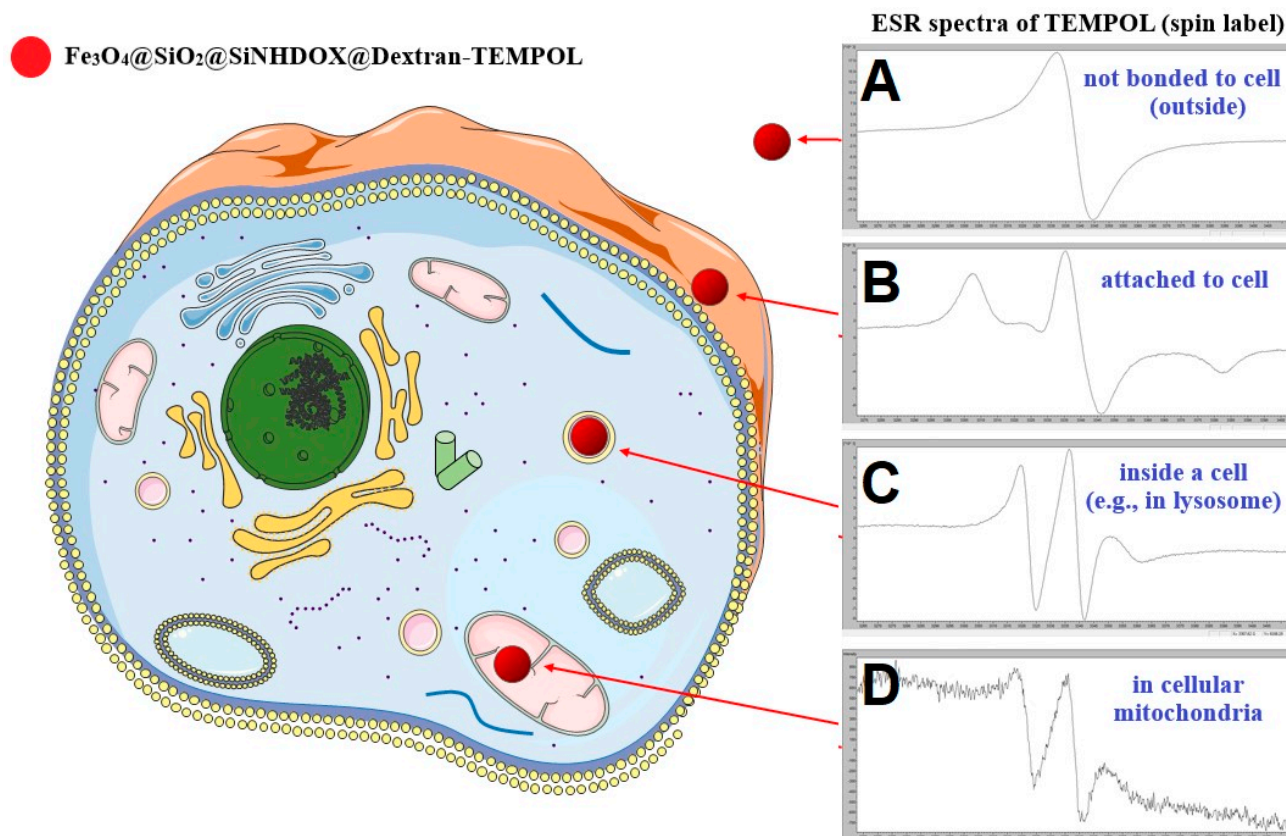


Figure 9. Changes in the structure and intensity of ESR spectra in the endocytosis process of the functionalized nanoparticles in a cell: (A)—ESR signal from the spin label not bonded to cells; (B)—the spin label attached to a cell; (C)—the spin label located inside cells (in organelles such as endosome or lysosome); (D)—the spin label probably present in cellular mitochondria. Adapted from [134], *International Journal of Molecular Sciences* (2020).

6. Perspectives for Future Studies

Over the years, the preparation of systems based on magnetite nanoparticles for the targeted delivery of active compounds has developed significantly in research laboratories. Through ongoing advancements in this research field, expertise has been acquired in synthesizing magnetite nanoparticles, focusing on methods and their adaptation to achieve nanoparticles of the desired shape and size. Different approaches have been developed to enhance the bioavailability of such nanosystems and protect them against aggregation. After extensive research experience, surface functionalization methods utilizing diverse ligands have been thoroughly refined. These advancements enhance targeted and controlled delivery, minimizing the systemic toxicity of active substances. It, in turn, allows for a reduction in drug doses while preserving the therapeutic efficacy. In isolated conditions, advanced DDSs show excellent responsiveness to several stimuli, such as pH, redox, or external magnetic field. Notably, the obtained nanocarriers are thoroughly characterized using numerous physicochemical methods (e.g., FTIR, XRD, SEM, TEM, VSM).

On the other hand, the nanocarrier's functionality is primarily assessed at the laboratory level under *in vitro* conditions, focusing on the impact of a single factor (e.g., *in vitro* release studies in different pH conditions or *in vitro* cytotoxicity studies against selected cancer cell lines). Therefore, the general knowledge about their interaction and transformation in multicomponent biological environments is limited. The impact of protein corona on diminishing targeted delivery to the tumor microenvironment is poorly comprehended. Additionally, the activity of the reticuloendothelial system, responsible for eliminating foreign materials from biological systems, could substantially contribute to diminishing the effectiveness of the nanocarrier. Therefore, based on the results obtained

on single-component isolated models, it is difficult to predict the behavior of materials after introduction into a living organism. The economic aspect is undoubtedly a significant barrier. However, from the scientific side, an important issue that could contribute to progress in this area is the development of analytical methods enabling the tracking and interpreting of interactions in multicomponent biological systems. The second aspect that demands further exploration to enhance the efficacy of clinical trials involves comprehending and adeptly monitoring the desorption process of active substances from nanocarriers within a targeted environment after cellular uptake. Finally, controlling magnetite-based nanoparticles using an external magnetic field as a medium to direct them to the targeted area also requires the development of suitable methods so that their effectiveness is not limited only to subcutaneous tissues. However, in the authors' opinion, despite the many challenges still facing the scientific community, further development of targeted DDSs based on magnetite NPs has excellent potential for practical implementation. The general achievements and challenges in research on magnetite-based NPs for targeted drug delivery are summarized in Figure 10.

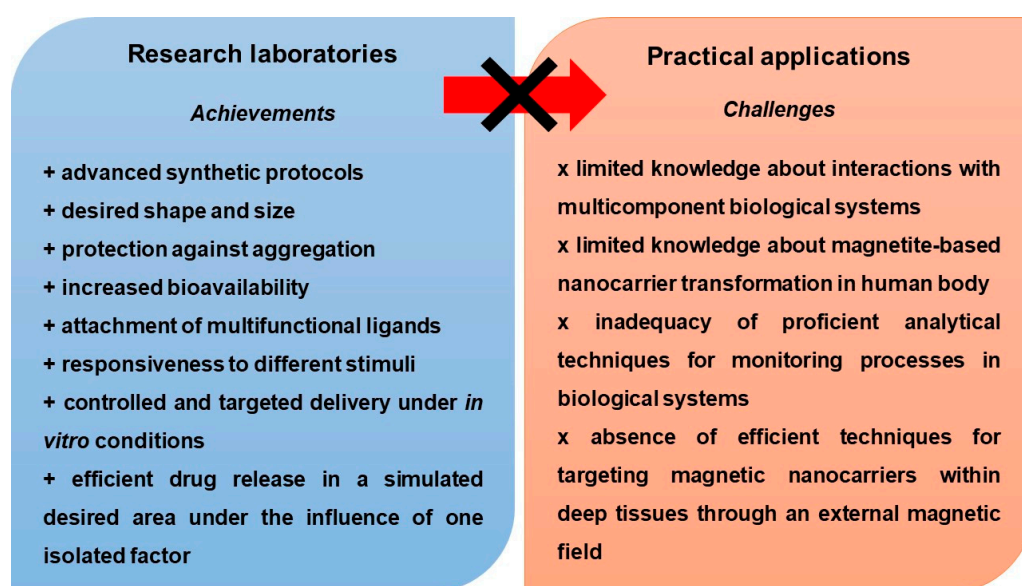


Figure 10. A schematic representation of achievements and challenges in research on magnetite-based nanoparticles for targeted drug delivery.

7. Conclusions

Original articles published over the last three years confirm high knowledge in designing systems with components enabling chemotherapeutic release in the desired areas of the tumor environment, with a limited impact on healthy cells. Despite various solutions, the synthesis products are well characterized based on many physicochemical techniques. Most of the investigated nanosystems demonstrate pH-responsiveness, and many with a disulfide bridge—redox-responsiveness. Most magnetic nanocarriers use folic acid as a targeting molecule and doxorubicin as an active agent. The primary, and frequently the sole, method for evaluating anticancer properties involves *in vitro* tests using cell lines. Significantly, their effectiveness is compared to the free drug and the carrier itself without adding the active components. They are used to characterize bioavailability, cytotoxicity, and cellular uptake. Conversely, *in vivo* studies in mice, which are less common, primarily evaluate tumor growth inhibition, the survival rate, and the impact of the drug-loaded nanocarrier on both cancer-affected and healthy organs. Numerous studies have successfully confirmed the selectivity of the drug loaded in the nanocarrier toward cancer cells, thus limiting its toxicity to healthy cells and enabling a reduction in the drug dose. Notably, many scientific papers highlight the various possibilities of using systems based on magnetite nanoparticles in cancer therapy and propose multifunctional materials, resulting in

a better therapeutic effect. First, a synergistic effect can be obtained by combining hyperthermia with chemotherapy. The temperature in the target area is increased by alternating magnetic field (MHT) or laser irradiation (PTT). Such systems can also perform a diagnostic function as negative contrast agents in MRI imaging. Cancer treatment often requires a combination of different therapies to increase effectiveness. Therefore, such multifunctional materials are especially in demand, and further development in this direction is required.

However, their clinical applications remain elusive despite extensive knowledge and the capability to design magnetic nanocarriers for targeted cancer therapy. Presumably, the knowledge about interactions between magnetic nanocarriers and biological systems is too limited, hindering overcoming this barrier. Analyzing the recent literature reports over the past three years reveals that the predominant approach employed in most of these studies involves utilizing fluorescence microscopy to investigate those interactions. Other less frequently used techniques include magnetic resonance imaging, flow cytometry, or confocal laser scanning microscopy. Unfortunately, few recent papers use more than one method to study this issue. Each of the methods discussed above has certain limitations. Therefore, indicating one appropriate technique for a given study is difficult. Moreover, analytical methods for better interpreting interactions occurring in biological systems should be developed. According to the authors, the optimal approach would be integrating multiple methods that provide insights into the interactions between magnetic nanoparticles and cells and enable comprehension of the factors responsible for the bioseparation of active agents from nanocarriers within the specified target region. It is worthwhile to explore the application of alternative techniques that have proven successful in studying magnetic nanoparticles in different fields but have not received adequate recognition in biomedical utilizations. Adopting this strategy could offer a pathway to understanding and overcoming challenges associated with implementing potential magnetite-based systems for practical drug delivery applications.

Author Contributions: Conceptualization, J.K.; writing—original draft preparation, J.K. and B.D.; writing—review and editing, J.K.; visualization, J.K.; supervision, J.K. All authors have read and agreed to the published version of the manuscript.

Funding: This research was funded by National Science Centre, Poland, grant number 2021/43/D/ST5/01190.

Institutional Review Board Statement: Not applicable.

Informed Consent Statement: Not applicable.

Data Availability Statement: Not applicable.

Conflicts of Interest: The authors declare no conflicts of interest.

References

1. Shabatina, T.I.; Vernaya, O.I.; Shabatin, V.P.; Melnikov, M.Y. Magnetic Nanoparticles for Biomedical Purposes: Modern Trends and Prospects. *Magnetochemistry* **2020**, *6*, 30. [[CrossRef](#)]
2. Rukhsar, M.; Ahmad, Z.; Rauf, A.; Zeb, H.; Ur-Rehman, M.; Hemeg, H.A. An Overview of Iron Oxide (Fe₃O₄) Nanoparticles: From Synthetic Strategies, Characterization to Antibacterial and Anticancer Applications. *Crystals* **2022**, *12*, 1809. [[CrossRef](#)]
3. Shabestari Khiabani, S.; Farshbaf, M.; Akbarzadeh, A.; Davaran, S. Magnetic Nanoparticles: Preparation Methods, Applications in Cancer Diagnosis and Cancer Therapy. *Artif. Cells Nanomed. Biotechnol.* **2017**, *45*, 6–17. [[CrossRef](#)] [[PubMed](#)]
4. Fatmawati, T.; Shiddiq, M.; Armynah, B.; Tahir, D. Synthesis Methods of Fe₃O₄ Nanoparticles for Biomedical Applications. *Chem. Eng. Technol.* **2023**, *46*, 2356–2366. [[CrossRef](#)]
5. Dudchenko, N.; Pawar, S.; Perelshtein, I.; Fixler, D. Magnetite Nanoparticles: Synthesis and Applications in Optics and Nanophotonics. *Materials* **2022**, *15*, 2601. [[CrossRef](#)]
6. Rao, M.S.; Rao, C.S.; Kumari, A.S. Synthesis, Stability, and Emission Analysis of Magnetite Nanoparticle-Based Biofuels. *J. Eng. Appl. Sci.* **2022**, *69*, 79. [[CrossRef](#)]
7. Kritika; Roy, I. Therapeutic Applications of Magnetic Nanoparticles: Recent Advances. *Mater. Adv.* **2022**, *3*, 7425–7444. [[CrossRef](#)]
8. Al-Madhagi, H.; Yazbik, V.; Abdelwahed, W.; Alchab, L. Magnetite Nanoparticle Co-Precipitation Synthesis, Characterization, and Applications: Mini Review. *BioNanoScience* **2023**, *13*, 853–859. [[CrossRef](#)]

9. Gallo-Cordova, A.; Almeida Streitwieser, D.; Del Puerto Morales, M.; Ovejero, J.G. Magnetic Iron Oxide Colloids for Environmental Applications. In *Colloids—Types, Preparation and Applications*; Nageeb Rashed, M., Ed.; IntechOpen: London, UK, 2021; ISBN 978-1-83962-969-3.
10. Ajinkya, N.; Yu, X.; Kaithal, P.; Luo, H.; Somani, P.; Ramakrishna, S. Magnetic Iron Oxide Nanoparticle (IONP) Synthesis to Applications: Present and Future. *Materials* **2020**, *13*, 4644. [[CrossRef](#)]
11. Montiel Schneider, M.G.; Martín, M.J.; Otarola, J.; Vakarelska, E.; Simeonov, V.; Lassalle, V.; Nedyalkova, M. Biomedical Applications of Iron Oxide Nanoparticles: Current Insights Progress and Perspectives. *Pharmaceutics* **2022**, *14*, 204. [[CrossRef](#)]
12. Khizar, S.; Ahmad, N.M.; Zine, N.; Jaffrezic-Renault, N.; Errachid-El-Salhi, A.; Elaissari, A. Magnetic Nanoparticles: From Synthesis to Theranostic Applications. *ACS Appl. Nano Mater.* **2021**, *4*, 4284–4306. [[CrossRef](#)]
13. Tran, H.-V.; Ngo, N.M.; Medhi, R.; Srinoi, P.; Liu, T.; Rittikulsittichai, S.; Lee, T.R. Multifunctional Iron Oxide Magnetic Nanoparticles for Biomedical Applications: A Review. *Materials* **2022**, *15*, 503. [[CrossRef](#)] [[PubMed](#)]
14. Campana, L.G.; Falci, C.; Basso, M.; Sieni, E.; Dughiero, F. Clinical Electrochemotherapy for Chest Wall Recurrence from Breast Cancer. In *Electroporation-Based Therapies for Cancer*; Elsevier: Amsterdam, The Netherlands, 2014; pp. 3–33. ISBN 978-1-907568-15-2.
15. Wagalgave, S.M.; Birajdar, S.S.; Malegaonkar, J.N.; Bhosale, S.V. Patented AIE Materials for Biomedical Applications. In *Progress in Molecular Biology and Translational Science*; Elsevier: Amsterdam, The Netherlands, 2021; Volume 185, pp. 199–223, ISBN 978-0-323-99604-4.
16. Gao, P.; Wang, H.; Cheng, Y. Strategies for Efficient Photothermal Therapy at Mild Temperatures: Progresses and Challenges. *Chin. Chem. Lett.* **2022**, *33*, 575–586. [[CrossRef](#)]
17. Chan, R.W.; Lau, J.Y.C.; Lam, W.W.; Lau, A.Z. Magnetic Resonance Imaging. In *Encyclopedia of Biomedical Engineering*; Elsevier: Amsterdam, The Netherlands, 2019; pp. 574–587, ISBN 978-0-12-805144-3.
18. Avasthi, A.; Caro, C.; Pozo-Torres, E.; Leal, M.P.; García-Martín, M.L. Magnetic Nanoparticles as MRI Contrast Agents. *Top. Curr. Chem.* **2020**, *378*, 40. [[CrossRef](#)] [[PubMed](#)]
19. Ezike, T.C.; Okpala, U.S.; Onoja, U.L.; Nwike, C.P.; Ezeako, E.C.; Okpara, O.J.; Okoroafor, C.C.; Eze, S.C.; Kalu, O.L.; Odoh, E.C.; et al. Advances in Drug Delivery Systems, Challenges and Future Directions. *Heliyon* **2023**, *9*, e17488. [[CrossRef](#)] [[PubMed](#)]
20. Vargason, A.M.; Anselmo, A.C.; Mitragotri, S. The Evolution of Commercial Drug Delivery Technologies. *Nat. Biomed. Eng.* **2021**, *5*, 951–967. [[CrossRef](#)]
21. Adepu, S.; Ramakrishna, S. Controlled Drug Delivery Systems: Current Status and Future Directions. *Molecules* **2021**, *26*, 5905. [[CrossRef](#)]
22. Sahini, M.G.; Banyikwa, A.T. Superparamagnetic Iron Oxide Nanoparticles for Drug Delivery Applications. In *Advanced and Modern Approaches for Drug Delivery*; Elsevier: Amsterdam, The Netherlands, 2023; pp. 817–850. ISBN 978-0-323-91668-4.
23. Anik, M.I.; Hossain, M.K.; Hossain, I.; Mahfuz, A.M.U.B.; Rahman, M.T.; Ahmed, I. Recent Progress of Magnetic Nanoparticles in Biomedical Applications: A Review. *Nano Sel.* **2021**, *2*, 1146–1186. [[CrossRef](#)]
24. Malhotra, N.; Lee, J.-S.; Liman, R.A.D.; Ruallo, J.M.S.; Villaflores, O.B.; Ger, T.-R.; Hsiao, C.-D. Potential Toxicity of Iron Oxide Magnetic Nanoparticles: A Review. *Molecules* **2020**, *25*, 3159. [[CrossRef](#)]
25. Frtús, A.; Smolková, B.; Uzhytchak, M.; Lunova, M.; Jirsa, M.; Kubinová, Š.; Dejneka, A.; Lunov, O. Analyzing the Mechanisms of Iron Oxide Nanoparticles Interactions with Cells: A Road from Failure to Success in Clinical Applications. *J. Control. Release* **2020**, *328*, 59–77. [[CrossRef](#)]
26. Wang, F.; Geng, J.; Qi, X.; Zhang, P.; Zhang, H.; He, X.; Li, Z.; Yu, R.; Li, J.; Li, B.; et al. Facile Solvothermal Synthesis of Monodisperse Superparamagnetic Mesoporous Fe₃O₄ Nanospheres for pH-Responsive Controlled Drug Delivery. *Colloids Surf. A* **2021**, *622*, 126643. [[CrossRef](#)]
27. Wang, F.; Qi, X.; Geng, J.; Liu, X.; Li, D.; Zhang, H.; Zhang, P.; He, X.; Li, B.; Li, Z.; et al. Template-Free Construction of Hollow Mesoporous Fe₃O₄ Nanospheres as Controlled Drug Delivery with Enhanced Drug Loading Capacity. *J. Mol. Liq.* **2022**, *347*, 118000. [[CrossRef](#)]
28. Yoon, H.-M.; Kang, M.-S.; Choi, G.-E.; Kim, Y.-J.; Bae, C.-H.; Yu, Y.-B.; Jeong, Y.-I. Stimuli-Responsive Drug Delivery of Doxorubicin Using Magnetic Nanoparticle Conjugated Poly(Ethylene Glycol)-g-Chitosan Copolymer. *Int. J. Mol. Sci.* **2021**, *22*, 13169. [[CrossRef](#)]
29. Wu, T.-C.; Lee, P.-Y.; Lai, C.-L.; Lai, C.-H. Synthesis of Multi-Functional Nano-Vectors for Target-Specific Drug Delivery. *Polymers* **2021**, *13*, 451. [[CrossRef](#)] [[PubMed](#)]
30. Hosny, N.M.; Abbass, M.; Ismail, F.; El-Din, H.M.N. Radiation Synthesis and Anticancer Drug Delivery of Poly(Acrylic Acid/Acrylamide) Magnetite Hydrogel. *Polym. Bull.* **2023**, *80*, 4573–4588. [[CrossRef](#)]
31. Javadian, S.; Najafi, K.; Sadrpoor, S.M.; Ektefa, F.; Dalir, N.; Nikkhah, M. Graphene Quantum Dots Based Magnetic Nanoparticles as a Promising Delivery System for Controlled Doxorubicin Release. *J. Mol. Liq.* **2021**, *331*, 115746. [[CrossRef](#)]
32. Karimi, S.; Namazi, H. A Photoluminescent Folic Acid-Derived Carbon Dot Functionalized Magnetic Dendrimer as a pH-Responsive Carrier for Targeted Doxorubicin Delivery. *New J. Chem.* **2021**, *45*, 6397–6405. [[CrossRef](#)]
33. Silva, A.S.; Diaz De Tuesta, J.L.; Sayuri Berberich, T.; Delezuk Inglez, S.; Bertão, A.R.; Çaha, I.; Deepak, F.L.; Bañobre-López, M.; Gomes, H.T. Doxorubicin Delivery Performance of Superparamagnetic Carbon Multi-Core Shell Nanoparticles: pH Dependence, Stability and Kinetic Insight. *Nanoscale* **2022**, *14*, 7220–7232. [[CrossRef](#)] [[PubMed](#)]
34. Demin, A.M.; Vakhrushev, A.V.; Valova, M.S.; Korolyova, M.A.; Uimin, M.A.; Minin, A.S.; Pozdina, V.A.; Byzov, I.V.; Tumashov, A.A.; Chistyakov, K.A.; et al. Effect of the Silica–Magnetite Nanocomposite Coating Functionalization on the Doxorubicin Sorption/Desorption. *Pharmaceutics* **2022**, *14*, 2271. [[CrossRef](#)]

35. Li, Y.; Dong, D.; Qu, Y.; Li, J.; Chen, S.; Zhao, H.; Zhang, Q.; Jiao, Y.; Fan, L.; Sun, D. A Multidrug Delivery Microrobot for the Synergistic Treatment of Cancer. *Small* **2023**, *19*, 2301889. [CrossRef]
36. Lee, H.; Park, S. Magnetically Actuated Helical Microrobot with Magnetic Nanoparticle Retrieval and Sequential Dual-Drug Release Abilities. *ACS Appl. Mater. Interfaces* **2023**, *15*, 27471–27485. [CrossRef]
37. Khasraw, M.; Bell, R.; Dang, C. Epirubicin: Is It like Doxorubicin in Breast Cancer? A Clinical Review. *Breast* **2012**, *21*, 142–149. [CrossRef]
38. Taheri-Kafrani, A.; Shirzadfar, H.; Abbasi Kajani, A.; Kudhair, B.K.; Jasim Mohammed, L.; Mohammadi, S.; Lotfi, F. Functionalized Graphene Oxide/Fe₃O₄ Nanocomposite: A Biocompatible and Robust Nanocarrier for Targeted Delivery and Release of Anticancer Agents. *J. Biotechnol.* **2021**, *331*, 26–36. [CrossRef] [PubMed]
39. Geyik, G.; Işıklan, N. Multi-Stimuli-Sensitive Superparamagnetic κ-Carrageenan Based Nanoparticles for Controlled 5-Fluorouracil Delivery. *Colloids Surf. A* **2022**, *634*, 127960. [CrossRef]
40. Ali, Z.; Sajid, M.; Ahmed, M.M.; Hanif, M.; Manzoor, S. Synthesis of Green Fluorescent Cross-Linked Molecularly Imprinted Polymer Bound with Anti-Cancerous Drug (Docetaxel) for Targeted Drug Delivery. *Polym. Bull.* **2024**, *81*, 679–696. [CrossRef]
41. Romdoni, Y.; Kadja, G.T.M.; Kitamoto, Y.; Khalil, M. Synthesis of Multifunctional Fe₃O₄@SiO₂-Ag Nanocomposite for Antibacterial and Anticancer Drug Delivery. *Appl. Surf. Sci.* **2023**, *610*, 155610. [CrossRef]
42. Bray, F.; Ferlay, J.; Soerjomataram, I.; Siegel, R.L.; Torre, L.A.; Jemal, A. Global Cancer Statistics 2018: GLOBOCAN Estimates of Incidence and Mortality Worldwide for 36 Cancers in 185 Countries. *CA Cancer J. Clin.* **2018**, *68*, 394–424. [CrossRef]
43. Kreis, K.; Plöthner, M.; Schmidt, T.; Seufert, R.; Schreeb, K.; Jahndel, V.; Maas, S.; Kuhlmann, A.; Zeidler, J.; Schramm, A. Healthcare Costs Associated with Breast Cancer in Germany: A Claims Data Analysis. *Eur. J. Health Econ.* **2020**, *21*, 451–464. [CrossRef]
44. Kurczewska, J. Chitosan-Based Nanoparticles with Optimized Parameters for Targeted Delivery of a Specific Anticancer Drug—A Comprehensive Review. *Pharmaceutics* **2023**, *15*, 503. [CrossRef]
45. Ferreira, L.L.; Oliveira, P.J.; Cunha-Oliveira, T. Epigenetics in Doxorubicin Cardiotoxicity. In *Pharmacoeugenetics*; Elsevier: Amsterdam, The Netherlands, 2019; pp. 837–846, ISBN 978-0-12-813939-4.
46. Ehsanimehr, S.; Moghadam, P.N.; Dehaen, W.; Irannejad, V.S. PEI Grafted Fe₃O₄@SiO₂@SBA-15 Labeled FA as a pH-Sensitive Mesoporous Magnetic and Biocompatible Nanocarrier for Targeted Delivery of Doxorubicin to MCF-7 Cell Line. *Colloids Surf. A* **2021**, *615*, 126302. [CrossRef]
47. Jalali, S.; Moghadam, P.N.; Shafiei-Irannejad, V. Synthesis of Magnetic Nanocarrier Conjugated by Folate Based on Tragacanth and In Vitro Investigation of Their Efficiency on Breast Cancer Cells. *Starch* **2023**, *75*, 2200092. [CrossRef]
48. Parvaresh, A.; Izadi, Z.; Nemati, H.; Derakhshankhah, H.; Jaymand, M. Redox- and pH-Responsive Alginate-Based Magnetic Hydrogel: “Smart” Drug Delivery and Protein Corona Studies. *J. Mol. Liq.* **2023**, *382*, 121990. [CrossRef]
49. Liu, Q.; Tan, Z.; Zheng, D.; Qiu, X. pH-Responsive Magnetic Fe₃O₄/Carboxymethyl Chitosan/Aminated Lignosulfonate Nanoparticles with Uniform Size for Targeted Drug Loading. *Int. J. Biol. Macromol.* **2023**, *225*, 1182–1192. [CrossRef] [PubMed]
50. Naghaviyan, A.; Hashemi-Moghaddam, H.; Zavareh, S.; Ebrahimi Verkiani, M.; Mueller, A. Synergistic Effect Evaluation of Magnetotherapy and a Cationic–Magnetic Nanocomposite Loaded with Doxorubicin for Targeted Drug Delivery to Breast Adenocarcinoma. *Mol. Pharm.* **2023**, *20*, 101–117. [CrossRef]
51. Radu, I.-C.; Mirica, A.-C.I.; Hudita, A.; Tanasa, E.; Iovu, H.; Zaharia, C.; Galateanu, B. Thermosensitive Behavior Defines the Features of Poly(N-Isopropylacrylamide)/Magnetite Nanoparticles for Cancer Management. *Appl. Sci.* **2023**, *13*, 4870. [CrossRef]
52. Bekaroğlu, M.G.; Kiriş, A.; Başer, H.N.; İşçi, S. Stabilizer Effect of Tumor-Targeting Ligands on the Drug Delivering Fe₃O₄ Nanoparticles. *Appl. Phys. A* **2023**, *129*, 182. [CrossRef]
53. Popova, V.; Poletaeva, Y.; Chubarov, A.; Dmitrienko, E. pH-Responsible Doxorubicin-Loaded Fe₃O₄@CaCO₃ Nanocomposites for Cancer Treatment. *Pharmaceutics* **2023**, *15*, 771. [CrossRef]
54. Markhulia, J.; Kekutia, S.; Mikelashvili, V.; Sanablidze, L.; Tsertsvadze, T.; Maisuradze, N.; Leladze, N.; Czigány, Z.; Almásy, L. Synthesis, Characterization, and In Vitro Cytotoxicity Evaluation of Doxorubicin-Loaded Magnetite Nanoparticles on Triple-Negative Breast Cancer Cell Lines. *Pharmaceutics* **2023**, *15*, 1758. [CrossRef] [PubMed]
55. Li, M.; Wu, J.; Lin, D.; Yang, J.; Jiao, N.; Wang, Y.; Liu, L. A Diatom-Based Biohybrid Microrobot with a High Drug-Loading Capacity and pH-Sensitive Drug Release for Target Therapy. *Acta Biomater.* **2022**, *154*, 443–453. [CrossRef]
56. Gong, D.; Celi, N.; Zhang, D.; Cai, J. Magnetic Biohybrid Microrobot Multimers Based on *Chlorella* Cells for Enhanced Targeted Drug Delivery. *ACS Appl. Mater. Interfaces* **2022**, *14*, 6320–6330. [CrossRef]
57. Zhu, Y.; Jia, H.; Jiang, Y.; Guo, Y.; Duan, Q.; Xu, K.; Shan, B.; Liu, X.; Chen, X.; Wu, F. A Red Blood Cell-derived Bionic Microrobot Capable of Hierarchically Adapting to Five Critical Stages in Systemic Drug Delivery. *Exploration* **2023**, 20230105. [CrossRef]
58. Gong, D.; Sun, L.; Li, X.; Zhang, W.; Zhang, D.; Cai, J. Micro/Nanofabrication, Assembly, and Actuation Based on Microorganisms: Recent Advances and Perspectives. *Small Struct.* **2023**, *4*, 2200356. [CrossRef]
59. Ramadan, I.; Nassar, M.Y.; Gomaa, A. In-Vitro Investigation of the Anticancer Efficacy of Carboplatin-Loaded Chitosan Nanocomposites Against Breast and Liver Cancer Cell Lines. *J. Polym. Environ.* **2023**, *31*, 1102–1115. [CrossRef]
60. Nie, Z.; Vahdani, Y.; Cho, W.C.; Bloukh, S.H.; Edis, Z.; Haghighat, S.; Falahati, M.; Kheradmandi, R.; Jaragh-Alhadad, L.A.; Sharifi, M. 5-Fluorouracil-Containing Inorganic Iron Oxide/Platinum Nanozymes with Dual Drug Delivery and Enzyme-like Activity for the Treatment of Breast Cancer. *Arab. J. Chem.* **2022**, *15*, 103966. [CrossRef]

61. Li, J.; Zhou, Y.; Yan, S.; Wu, W.; Sharifi, M. Core-Shell Iron Oxide-Platinum@metal Organic Framework/Epirubicin Nanospheres: Synthesis, Characterization and Anti-Breast Cancer Activity. *Arab. J. Chem.* **2023**, *16*, 105229. [[CrossRef](#)]
62. Parsa, F.; Setoodehkhah, M.; Atyabi, S.M. Loading and Release Study of Ciprofloxacin from Silica-Coated Magnetite Modified by Iron-Based Metal-Organic Framework (MOF) as a Nonocarrier in Targeted Drug Delivery System. *Inorg. Chem. Commun.* **2023**, *155*, 111056. [[CrossRef](#)]
63. Khodadadi, E.; Mahjoub, S.; Arabi, M.S.; Najafzadehvarzi, H.; Nasirian, V. Fabrication and Evaluation of Aptamer-Conjugated Paclitaxel-Loaded Magnetic Nanoparticles for Targeted Therapy on Breast Cancer Cells. *Mol. Biol. Rep.* **2021**, *48*, 2105–2116. [[CrossRef](#)] [[PubMed](#)]
64. Cadena Castro, D.; Gatti, G.; Martín, S.E.; Uberman, P.M.; García, M.C. Promising Tamoxifen-Loaded Biocompatible Hybrid Magnetic Nanoplatforms against Breast Cancer Cells: Synthesis, Characterization and Biological Evaluation. *New J. Chem.* **2021**, *45*, 4032–4045. [[CrossRef](#)]
65. Karimi, S.; Namazi, H. Synthesis of Folic Acid-Conjugated Glycodendrimer with Magnetic β -Cyclodextrin Core as a pH-Responsive System for Tumor-Targeted Co-Delivery of Doxorubicin and Curcumin. *Colloids Surf. A* **2021**, *627*, 127205. [[CrossRef](#)]
66. Ahmadi, F.; Akbari, J.; Saeedi, M.; Seyedabadi, M.; Ebrahimnejad, P.; Ghasemi, S.; Nokhodchi, A. Efficient Synergistic Combination Effect of Curcumin with Piperine by Polymeric Magnetic Nanoparticles for Breast Cancer Treatment. *J. Drug Deliv. Sci. Technol.* **2023**, *86*, 104624. [[CrossRef](#)]
67. Seyyedi Zadeh, E.; Ghanbari, N.; Salehi, Z.; Derakhti, S.; Amoabediny, G.; Akbari, M.; Asadi Tokmedash, M. Smart pH-Responsive Magnetic Graphene Quantum Dots Nanocarriers for Anticancer Drug Delivery of Curcumin. *Mater. Chem. Phys.* **2023**, *297*, 127336. [[CrossRef](#)]
68. Matiyani, M.; Rana, A.; Pal, M.; Rana, S.; Melkani, A.B.; Sahoo, N.G. Polymer Grafted Magnetic Graphene Oxide as a Potential Nanocarrier for pH-Responsive Delivery of Sparingly Soluble Quercetin against Breast Cancer Cells. *RSC Adv.* **2022**, *12*, 2574–2588. [[CrossRef](#)] [[PubMed](#)]
69. Yang, W.-S.; Zeng, X.-F.; Liu, Z.-N.; Zhao, Q.-H.; Tan, Y.-T.; Gao, J.; Li, H.-L.; Xiang, Y.-B. Diet and Liver Cancer Risk: A Narrative Review of Epidemiological Evidence. *Br. J. Nutr.* **2020**, *124*, 330–340. [[CrossRef](#)] [[PubMed](#)]
70. Wang, L.; Liang, L.; Shi, S.; Wang, C. Study on the Application of Doxorubicin-Loaded Magnetic Nanodrugs in Targeted Therapy of Liver Cancer. *Appl. Bionics Biomech.* **2022**, *2022*, 2756459. [[CrossRef](#)]
71. Mdlovu, N.V.; Lin, K.-S.; Weng, M.-T.; Lin, Y.-S. Design of Doxorubicin Encapsulated pH-/Thermo-Responsive and Cationic Shell-Crosslinked Magnetic Drug Delivery System. *Colloids Surf. B* **2022**, *209*, 112168. [[CrossRef](#)]
72. Carrera Espinoza, M.J.; Lin, K.-S.; Weng, M.-T.; Kunene, S.C.; Lin, Y.-S.; Liu, S.-Y. Magnetic Boron Nitride Nanosheets-Based on pH-Responsive Smart Nanocarriers for the Delivery of Doxorubicin for Liver Cancer Treatment. *Colloids Surf. B* **2023**, *222*, 113129. [[CrossRef](#)]
73. Wang, X.; Ma, Q.; Wen, C.; Gong, T.; Li, J.; Liang, W.; Li, M.; Wang, Y.; Guo, R. Folic Acid and Deoxycholic Acid Derivative Modified Fe₃O₄ Nanoparticles for Efficient pH-Dependent Drug Release and Multi-Targeting against Liver Cancer Cells. *RSC Adv.* **2021**, *11*, 39804–39812. [[CrossRef](#)]
74. Chai, J.; Ma, Y.; Guo, T.; He, Y.; Wang, G.; Si, F.; Geng, J.; Qi, X.; Chang, G.; Ren, Z.; et al. Assembled Fe₃O₄ Nanoparticles on Zn Al LDH Nanosheets as a Biocompatible Drug Delivery Vehicle for pH-Responsive Drug Release and Enhanced Anticancer Activity. *Appl. Clay Sci.* **2022**, *228*, 106630. [[CrossRef](#)]
75. Ebadi, M.; Rifqi Md Zain, A.; Tengku Abdul Aziz, T.H.; Mohammadi, H.; Tee, C.A.T.; Rahimi Yusop, M. Formulation and Characterization of Fe₃O₄@PEG Nanoparticles Loaded Sorafenib; Molecular Studies and Evaluation of Cytotoxicity in Liver Cancer Cell Lines. *Polymers* **2023**, *15*, 971. [[CrossRef](#)] [[PubMed](#)]
76. Iacobazzi, R.M.; Vischio, F.; Arduino, I.; Canepa, F.; Laquintana, V.; Notarnicola, M.; Scavo, M.P.; Bianco, G.; Fanizza, E.; Lopodota, A.A.; et al. Magnetic Implants In Vivo Guiding Sorafenib Liver Delivery by Superparamagnetic Solid Lipid Nanoparticles. *J. Colloid Interface Sci.* **2022**, *608*, 239–254. [[CrossRef](#)]
77. Ebadi, M.; Bullo, S.; Buskaran, K.; Hussein, M.Z.; Fakurazi, S.; Pastorin, G. Dual-Functional Iron Oxide Nanoparticles Coated with Polyvinyl Alcohol/5-Fluorouracil/Zinc-Aluminium-Layered Double Hydroxide for a Simultaneous Drug and Target Delivery System. *Polymers* **2021**, *13*, 855. [[CrossRef](#)]
78. Ibrahim, S.; Baig, B.; Hisaindee, S.; Darwish, H.; Abdel-Ghany, A.; El-Maghraby, H.; Amin, A.; Greish, Y. Development and Evaluation of Crocetin-Functionalized Pegylated Magnetite Nanoparticles for Hepatocellular Carcinoma. *Molecules* **2023**, *28*, 2882. [[CrossRef](#)]
79. Mansour, W.; El Fedawy, S.F.; Atta, S.A.; Zarie, R.M.; Fouad, N.T.A.; Maher, S.; Hussein, T.M.; Abdel Aziz, D.M.; Kamel, M. Targeted Therapy for HCC Using Dumbbell-like Nanoparticles Conjugated to Monoclonal Antibodies against VEGF and Cancer Stem Cell Receptors in Mice. *Cancer Nano.* **2023**, *14*, 14. [[CrossRef](#)]
80. Yusefi, M.; Lee-Kiun, M.S.; Shameli, K.; Teow, S.-Y.; Ali, R.R.; Siew, K.-K.; Chan, H.-Y.; Wong, M.M.-T.; Lim, W.-L.; Kuča, K. 5-Fluorouracil Loaded Magnetic Cellulose Bionanocomposites for Potential Colorectal Cancer Treatment. *Carbohydr. Polym.* **2021**, *273*, 118523. [[CrossRef](#)] [[PubMed](#)]
81. Mirzaghavami, P.S.; Khoei, S.; Khoei, S.; Shirvalilou, S. Folic Acid-Conjugated Magnetic Triblock Copolymer Nanoparticles for Dual Targeted Delivery of 5-Fluorouracil to Colon Cancer Cells. *Cancer Nano.* **2022**, *13*, 12. [[CrossRef](#)]

82. Shirvalilou, S.; Khoei, S.; Khoei, S.; Karimi, M.R.; Sadri, E.; Shirvaliloo, M. Targeted Magnetochemotherapy Modified by 5-Fu-Loaded Thermally on/off Switching Nanoheaters for the Eradication of CT26 Murine Colon Cancer by Inducing Apoptotic and Autophagic Cell Death. *Cancer Nano*. **2023**, *14*, 11. [[CrossRef](#)]
83. Farmanbar, N.; Mohseni, S.; Darroudi, M. Green Synthesis of Chitosan-Coated Magnetic Nanoparticles for Drug Delivery of Oxaliplatin and Irinotecan against Colorectal Cancer Cells. *Polym. Bull.* **2022**, *79*, 10595–10613. [[CrossRef](#)]
84. Zhu, H.; Zhang, L.; Kou, F.; Zhao, J.; Lei, J.; He, J. Targeted Therapeutic Effects of Oral Magnetically Driven Pectin Nanoparticles Containing Chlorogenic Acid on Colon Cancer. *Particuology* **2024**, *84*, 53–59. [[CrossRef](#)]
85. Siegel, R.L.; Miller, K.D.; Jemal, A. Cancer Statistics, 2019. *CA Cancer J. Clin.* **2019**, *69*, 7–34. [[CrossRef](#)]
86. Darroudi, M.; Nazari, S.E.; Asgharzadeh, F.; Khalili-Tanha, N.; Khalili-Tanha, G.; Dehghani, T.; Karimzadeh, M.; Maftooh, M.; Fern, G.A.; Avan, A.; et al. Fabrication and Application of Cisplatin-Loaded Mesoporous Magnetic Nanobiocomposite: A Novel Approach to Smart Cervical Cancer Chemotherapy. *Cancer Nano*. **2022**, *13*, 36. [[CrossRef](#)]
87. Ramezani Farani, M.; Azarian, M.; Heydari Sheikh Hossein, H.; Abdolvahabi, Z.; Mohammadi Abgarmi, Z.; Moradi, A.; Mousavi, S.M.; Ashrafizadeh, M.; Makvandi, P.; Saeb, M.R.; et al. Folic Acid-Adorned Curcumin-Loaded Iron Oxide Nanoparticles for Cervical Cancer. *ACS Appl. Bio Mater.* **2022**, *5*, 1305–1318. [[CrossRef](#)]
88. Zhao, Q.; Xie, P.; Li, X.; Wang, Y.; Zhang, Y.; Wang, S. Magnetic Mesoporous Silica Nanoparticles Mediated Redox and pH Dual-Responsive Target Drug Delivery for Combined Magnetothermal Therapy and Chemotherapy. *Colloids Surf. A* **2022**, *648*, 129359. [[CrossRef](#)]
89. Amiryaghoubi, N.; Abdolahinia, E.D.; Nakhband, A.; Aslzad, S.; Fathi, M.; Barar, J.; Omid, Y. Smart Chitosan–Folate Hybrid Magnetic Nanoparticles for Targeted Delivery of Doxorubicin to Osteosarcoma Cells. *Colloids Surf. B* **2022**, *220*, 112911. [[CrossRef](#)]
90. Sabouri, Z.; Labbaf, S.; Karimzadeh, F.; Baharlou-Houreh, A.; McFarlane, T.V.; Esfahani, M.H.N. Fe₃O₄/Bioactive Glass Nanostructure: A Promising Therapeutic Platform for Osteosarcoma Treatment. *Biomed. Mater.* **2021**, *16*, 035016. [[CrossRef](#)] [[PubMed](#)]
91. Niu, G.; Yousefi, B.; Qujeq, D.; Marjani, A.; Asadi, J.; Wang, Z.; Mir, S.M. Melatonin and Doxorubicin Co-Delivered via a Functionalized Graphene-Dendrimeric System Enhances Apoptosis of Osteosarcoma Cells. *Mater. Sci. Eng. C* **2021**, *119*, 111554. [[CrossRef](#)] [[PubMed](#)]
92. Puiu, R.A.; Balaure, P.C.; Constantinescu, E.; Grumezescu, A.M.; Andronesu, E.; Oprea, O.-C.; Vasile, B.S.; Grumezescu, V.; Negut, I.; Nica, I.C.; et al. Anti-Cancer Nanopowders and MAPLE-Fabricated Thin Films Based on SPIONs Surface Modified with Paclitaxel Loaded β -Cyclodextrin. *Pharmaceutics* **2021**, *13*, 1356. [[CrossRef](#)] [[PubMed](#)]
93. Li, D.; Fan, Y.; Liu, M.; Huang, S.; Wang, S. The Effect of Using Albumin-Perfluorohexane/Cisplatin-Magnetite Nanoparticles Produced by Hydrothermal Method against Gastric Cancer Cells through Combination Therapy. *Arab. J. Chem.* **2023**, *16*, 104758. [[CrossRef](#)]
94. Al-Obaidy, R.; Haider, A.J.; Al-Musawi, S.; Arsad, N. Targeted Delivery of Paclitaxel Drug Using Polymer-Coated Magnetic Nanoparticles for Fibrosarcoma Therapy: In Vitro and In Vivo Studies. *Sci. Rep.* **2023**, *13*, 3180. [[CrossRef](#)] [[PubMed](#)]
95. Khalil, M.; Haq, E.A.; Dwiranti, A.; Prasedya, E.S.; Kitamoto, Y. Bifunctional Folic-Conjugated Aspartic-Modified Fe₃O₄ Nanocarriers for Efficient Targeted Anticancer Drug Delivery. *RSC Adv.* **2022**, *12*, 4961–4971. [[CrossRef](#)]
96. Dhavale, R.P.; Dhavale, R.P.; Sahoo, S.C.; Kollu, P.; Jadhav, S.U.; Patil, P.S.; Dongale, T.D.; Chougale, A.D.; Patil, P.B. Chitosan Coated Magnetic Nanoparticles as Carriers of Anticancer Drug Telmisartan: pH-Responsive Controlled Drug Release and Cytotoxicity Studies. *J. Phys. Chem. Solids* **2021**, *148*, 109749. [[CrossRef](#)]
97. Takke, A.; Shende, P. Magnetic-Core-Based Silibinin Nanopolymeric Carriers for the Treatment of Renal Cell Cancer. *Life Sci.* **2021**, *275*, 119377. [[CrossRef](#)]
98. Jahanban-Esfahlan, R.; Soleimani, K.; Derakhshankhah, H.; Haghshenas, B.; Rezaei, A.; Massoumi, B.; Farnudiyan-Habibi, A.; Samadian, H.; Jaymand, M. Multi-Stimuli-Responsive Magnetic Hydrogel Based on Tragacanth Gum as a De Novo Nanosystem for Targeted Chemo/Hyperthermia Treatment of Cancer. *J. Mater. Res.* **2021**, *36*, 858–869. [[CrossRef](#)]
99. Soleimani, K.; Arkan, E.; Derakhshankhah, H.; Haghshenas, B.; Jahanban-Esfahlan, R.; Jaymand, M. A Novel Bioreducible and pH-Responsive Magnetic Nanohydrogel Based on β -Cyclodextrin for Chemo/Hyperthermia Therapy of Cancer. *Carbohydr. Polym.* **2021**, *252*, 117229. [[CrossRef](#)]
100. Tsai, L.-H.; Young, T.-H.; Yen, C.-H.; Yao, W.-C.; Chang, C.-H. Intratumoral Thermo-Chemotherapeutic Alginate Hydrogel Containing Doxorubicin Loaded PLGA Nanoparticle and Heating Agent. *Int. J. Biol. Macromol.* **2023**, *251*, 126221. [[CrossRef](#)]
101. Gong, T.; Wang, X.; Zhu, H.; Wen, C.; Ma, Q.; Li, X.; Li, M.; Guo, R.; Liang, W. Folic Acid–Maltodextrin Polymer Coated Magnetic Graphene Oxide as a NIR-Responsive Nano-Drug Delivery System for Chemo-Photothermal Synergistic Inhibition of Tumor Cells. *RSC Adv.* **2023**, *13*, 12609–12617. [[CrossRef](#)]
102. Liu, X.; Wang, C.; Wang, X.; Tian, C.; Shen, Y.; Zhu, M. A Dual-Targeting Fe₃O₄@C/ZnO-DOX-FA Nanoplatform with pH-Responsive Drug Release and Synergetic Chemo-Photothermal Antitumor In Vitro and In Vivo. *Mater. Sci. Eng. C* **2021**, *118*, 111455. [[CrossRef](#)] [[PubMed](#)]
103. Ma, H.; Yu, G.; Cheng, J.; Song, L.; Zhou, Z.; Zhao, Y.; Zhao, Q.; Liu, L.; Wei, X.; Yang, M. Design of an Injectable Magnetic Hydrogel Based on the Tumor Microenvironment for Multimodal Synergistic Cancer Therapy. *Biomacromolecules* **2023**, *24*, 868–885. [[CrossRef](#)] [[PubMed](#)]
104. Wen, C.; Cheng, R.; Gong, T.; Huang, Y.; Li, D.; Zhao, X.; Yu, B.; Su, D.; Song, Z.; Liang, W. β -Cyclodextrin-Cholic Acid-Hyaluronic Acid Polymer Coated Fe₃O₄-Graphene Oxide Nanohybrids as Local Chemo-Photothermal Synergistic Agents for Enhanced Liver Tumor Therapy. *Colloids Surf. B* **2021**, *199*, 111510. [[CrossRef](#)] [[PubMed](#)]

105. Işıklan, N.; Hussien, N.A.; Türk, M. Hydroxypropyl Cellulose Functionalized Magnetite Graphene Oxide Nanobiocomposite for Chemo/Photothermal Therapy. *Colloids Surf. A* **2023**, *656*, 130322. [[CrossRef](#)]
106. Hu, W.; Qi, Q.; Hu, H.; Wang, C.; Zhang, Q.; Zhang, Z.; Zhao, Y.; Yu, X.; Guo, M.; Du, S.; et al. Fe₃O₄ Liposome for Photothermal/Chemo-Synergistic Inhibition of Metastatic Breast Tumor. *Colloids Surf. A* **2022**, *634*, 127921. [[CrossRef](#)]
107. Xia, Y.; Xu, R.; Ye, S.; Yan, J.; Kumar, P.; Zhang, P.; Zhao, X. Microfluidic Formulation of Curcumin-Loaded Multiresponsive Gelatin Nanoparticles for Anticancer Therapy. *ACS Biomater. Sci. Eng.* **2023**, *9*, 3402–3413. [[CrossRef](#)] [[PubMed](#)]
108. Liu, N.; Wu, L.; Zuo, W.; Lin, Q.; Liu, J.; Jin, Q.; Xiao, Z.; Chen, L.; Zhao, Y.; Zhou, J.; et al. pH/Thermal-Sensitive Nanoplatfom Capable of On-Demand Specific Release to Potentiate Drug Delivery and Combinational Hyperthermia/Chemo/Chemodynamic Therapy. *ACS Appl. Mater. Interfaces* **2022**, *14*, 29668–29678. [[CrossRef](#)] [[PubMed](#)]
109. Zhang, X.; Wei, P.; Wang, Z.; Zhao, Y.; Xiao, W.; Bian, Y.; Liang, D.; Lin, Q.; Song, W.; Jiang, W.; et al. Herceptin-Conjugated DOX-Fe₃O₄/P(NIPAM-AA-MAPEG) Nanogel System for HER2-Targeted Breast Cancer Treatment and Magnetic Resonance Imaging. *ACS Appl. Mater. Interfaces* **2022**, *14*, 15956–15969. [[CrossRef](#)] [[PubMed](#)]
110. Fattahi Nafchi, R.; Ahmadi, R.; Heydari, M.; Rahimpour, M.R.; Molaei, M.J.; Unsworth, L. In Vitro Study: Synthesis and Evaluation of Fe₃O₄/CQD Magnetic/Fluorescent Nanocomposites for Targeted Drug Delivery, MRI, and Cancer Cell Labeling Applications. *Langmuir* **2022**, *38*, 3804–3816. [[CrossRef](#)] [[PubMed](#)]
111. Zohreh, N.; Rastegaran, Z.; Hosseini, S.H.; Akhlaghi, M.; Istrate, C.; Busuioc, C. pH-Triggered Intracellular Release of Doxorubicin by a Poly(Glycidyl Methacrylate)-Based Double-Shell Magnetic Nanocarrier. *Mater. Sci. Eng. C* **2021**, *118*, 111498. [[CrossRef](#)]
112. Hasani, M.; Jafari, S.; Akbari Javar, H.; Abdollahi, H.; Rashidzadeh, H. Cell-Penetrating Peptidic GRP78 Ligand-Conjugated Iron Oxide Magnetic Nanoparticles for Tumor-Targeted Doxorubicin Delivery and Imaging. *ACS Appl. Bio Mater.* **2023**, *6*, 1019–1031. [[CrossRef](#)]
113. García-García, G.; Caro, C.; Fernández-Álvarez, F.; García-Martín, M.L.; Arias, J.L. Multi-Stimuli-Responsive Chitosan-Functionalized Magnetite/Poly(ϵ -Caprolactone) Nanoparticles as Theranostic Platforms for Combined Tumor Magnetic Resonance Imaging and Chemotherapy. *Nanomed. Nanotechnol. Biol. Med.* **2023**, *52*, 102695. [[CrossRef](#)]
114. Wang, X.; Qi, Y.; Hu, Z.; Jiang, L.; Pan, F.; Xiang, Z.; Xiong, Z.; Jia, W.; Hu, J.; Lu, W. Fe₃O₄@PVP@DOX Magnetic Vortex Hybrid Nanostructures with Magnetic-Responsive Heating and Controlled Drug Delivery Functions for Precise Medicine of Cancers. *Adv. Compos. Hybrid Mater.* **2022**, *5*, 1786–1798. [[CrossRef](#)]
115. Yusefi, M.; Shameli, K.; Hedayatnasab, Z.; Teow, S.-Y.; Ismail, U.N.; Azlan, C.A.; Rasit Ali, R. Green Synthesis of Fe₃O₄ Nanoparticles for Hyperthermia, Magnetic Resonance Imaging and 5-Fluorouracil Carrier in Potential Colorectal Cancer Treatment. *Res. Chem. Intermed.* **2021**, *47*, 1789–1808. [[CrossRef](#)]
116. Zhang, C.; Wang, M.; Zhang, J.; Zou, B.; Wang, Y. Self-Template Synthesis of Mesoporous and Biodegradable Fe₃O₄ Nanospheres as Multifunctional Nanoplatfom for Cancer Therapy. *Colloids Surf. B* **2023**, *229*, 113467. [[CrossRef](#)]
117. Wang, H.; Xu, S.; Fan, D.; Geng, X.; Zhi, G.; Wu, D.; Shen, H.; Yang, F.; Zhou, X.; Wang, X. Multifunctional Microcapsules: A Theranostic Agent for US/MR/PAT Multi-Modality Imaging and Synergistic Chemo-Photothermal Osteosarcoma Therapy. *Bioact. Mater.* **2022**, *7*, 453–465. [[CrossRef](#)]
118. Zablotskii, V.; Polyakova, T.; Dejneka, A. Effects of High Magnetic Fields on the Diffusion of Biologically Active Molecules. *Cells* **2021**, *11*, 81. [[CrossRef](#)]
119. Yadegari Dehkordi, S.; Firoozabadi, S.M.; Forouzandeh Moghadam, M.; Shankayi, Z. Endocytosis Induction by High-Pulsed Magnetic Fields to Overcome Cell Membrane Barrier and Improve Chemotherapy Efficiency. *Electromagn. Biol. Med.* **2021**, *40*, 438–445. [[CrossRef](#)]
120. Alromi, D.; Madani, S.; Seifalian, A. Emerging Application of Magnetic Nanoparticles for Diagnosis and Treatment of Cancer. *Polymers* **2021**, *13*, 4146. [[CrossRef](#)] [[PubMed](#)]
121. Krzyminiowski, R.; Dobosz, B.; Schroeder, G.; Kurczewska, J. The Principles of a New Method, MNF-3D, for Concentration of Magnetic Particles in Three-Dimensional Space. *Meas. J. Int. Meas. Confed.* **2017**, *112*, 137–140. [[CrossRef](#)]
122. Dobosz, B.; Schroeder, G.; Kurczewska, J. Comments on “The Principles of a New Method, MNF-3D, for Concentration of Magnetic Particles in Three-Dimensional Space”. *Measurement* **2023**, *218*, 113146. [[CrossRef](#)]
123. Auría-Soro, C.; Nesma, T.; Juanes-Velasco, P.; Landeira-Viñuela, A.; Fidalgo-Gomez, H.; Acebes-Fernandez, V.; Gongora, R.; Almendral Parra, M.J.; Manzano-Roman, R.; Fuentes, M. Interactions of Nanoparticles and Biosystems: Microenvironment of Nanoparticles and Biomolecules in Nanomedicine. *Nanomaterials* **2019**, *9*, 1365. [[CrossRef](#)]
124. Abarca-Cabrera, L.; Fraga-García, P.; Berensmeier, S. Bio-Nano Interactions: Binding Proteins, Polysaccharides, Lipids and Nucleic Acids onto Magnetic Nanoparticles. *Biomater. Res.* **2021**, *25*, 12. [[CrossRef](#)] [[PubMed](#)]
125. Malatesta, M. Transmission Electron Microscopy as a Powerful Tool to Investigate the Interaction of Nanoparticles with Subcellular Structures. *Int. J. Mol. Sci.* **2021**, *22*, 12789. [[CrossRef](#)]
126. Rennick, J.J.; Johnston, A.P.R.; Parton, R.G. Key Principles and Methods for Studying the Endocytosis of Biological and Nanoparticle Therapeutics. *Nat. Nanotechnol.* **2021**, *16*, 266–276. [[CrossRef](#)]
127. Sousa De Almeida, M.; Susnik, E.; Drasler, B.; Taladriz-Blanco, P.; Petri-Fink, A.; Rothen-Rutishauser, B. Understanding Nanoparticle Endocytosis to Improve Targeting Strategies in Nanomedicine. *Chem. Soc. Rev.* **2021**, *50*, 5397–5434. [[CrossRef](#)] [[PubMed](#)]
128. FitzGerald, L.I.; Johnston, A.P.R. It’s What’s on the Inside That Counts: Techniques for Investigating the Uptake and Recycling of Nanoparticles and Proteins in Cells. *J. Colloid Interface Sci.* **2021**, *587*, 64–78. [[CrossRef](#)]

129. Nowak-Jary, J.; Machnicka, B. In Vivo Biodistribution and Clearance of Magnetic Iron Oxide Nanoparticles for Medical Applications. *Int. J. Nanomed.* **2023**, *18*, 4067–4100. [[CrossRef](#)]
130. Spoială, A.; Ilie, C.-I.; Motelica, L.; Fikai, D.; Semenescu, A.; Oprea, O.-C.; Fikai, A. Smart Magnetic Drug Delivery Systems for the Treatment of Cancer. *Nanomaterials* **2023**, *13*, 876. [[CrossRef](#)] [[PubMed](#)]
131. Huang, H.; Zhang, Z.; Li, G. A Review of Magnetic Nanoparticle-Based Surface-Enhanced Raman Scattering Substrates for Bioanalysis: Morphology, Function and Detection Application. *Biosensors* **2022**, *13*, 30. [[CrossRef](#)]
132. Ovcherenko, S.S.; Chinak, O.A.; Chechushkov, A.V.; Dobrynin, S.A.; Kirilyuk, I.A.; Krumkacheva, O.A.; Richter, V.A.; Bagryanskaya, E.G. Uptake of Cell-Penetrating Peptide RL2 by Human Lung Cancer Cells: Monitoring by Electron Paramagnetic Resonance and Confocal Laser Scanning Microscopy. *Molecules* **2021**, *26*, 5442. [[CrossRef](#)] [[PubMed](#)]
133. Krzyminiewski, R.; Dobosz, B.; Schroeder, G.; Kurczewska, J. ESR as a Monitoring Method of the Interactions between TEMPO-Functionalized Magnetic Nanoparticles and Yeast Cells. *Sci. Rep.* **2019**, *9*, 18733. [[CrossRef](#)]
134. Krzyminiewski, R.; Dobosz, B.; Krist, B.; Schroeder, G.; Kurczewska, J.; Bluysen, H.A.R. ESR Method in Monitoring of Nanoparticle Endocytosis in Cancer Cells. *Int. J. Mol. Sci.* **2020**, *21*, 4388. [[CrossRef](#)]
135. Shashni, B.; Nagasaki, Y. Newly Developed Self-Assembling Antioxidants as Potential Therapeutics for the Cancers. *J. Pers. Med.* **2021**, *11*, 92. [[CrossRef](#)]
136. Arfin, S.; Jha, N.K.; Jha, S.K.; Kesari, K.K.; Ruokolainen, J.; Roychoudhury, S.; Rathi, B.; Kumar, D. Oxidative Stress in Cancer Cell Metabolism. *Antioxidants* **2021**, *10*, 642. [[CrossRef](#)]
137. Dobosz, B.; Krzyminiewski, R.; Kucińska, M.; Murias, M.; Schroeder, G.; Kurczewska, J. Spin Probes as Scavengers of Free Radicals in Cells. *Appl. Sci.* **2022**, *12*, 7999. [[CrossRef](#)]

Disclaimer/Publisher's Note: The statements, opinions and data contained in all publications are solely those of the individual author(s) and contributor(s) and not of MDPI and/or the editor(s). MDPI and/or the editor(s) disclaim responsibility for any injury to people or property resulting from any ideas, methods, instructions or products referred to in the content.